Imaging, Tomography and Coherent Diffraction at Diamond

Ian Robinson
Diamond Light Source
University College, London

ICI, Redcar
June 2007

Outline

- Diamond's new capabilities
- Tomography and Phase Contrast
- Typical results
- Angular Rheology of paint
- Inversion of Coherent X-ray Diffraction

diamond

Acknowlegements

- Christoph Rau, Diamond
- Wenbing Yun, Xradia Inc
- Meng Liang, University of Illinois
- Ross Harder, UCL
- Paul Fenter, Yong Chu, Argonne

diamond

Diamond Light Source in Oct 2005

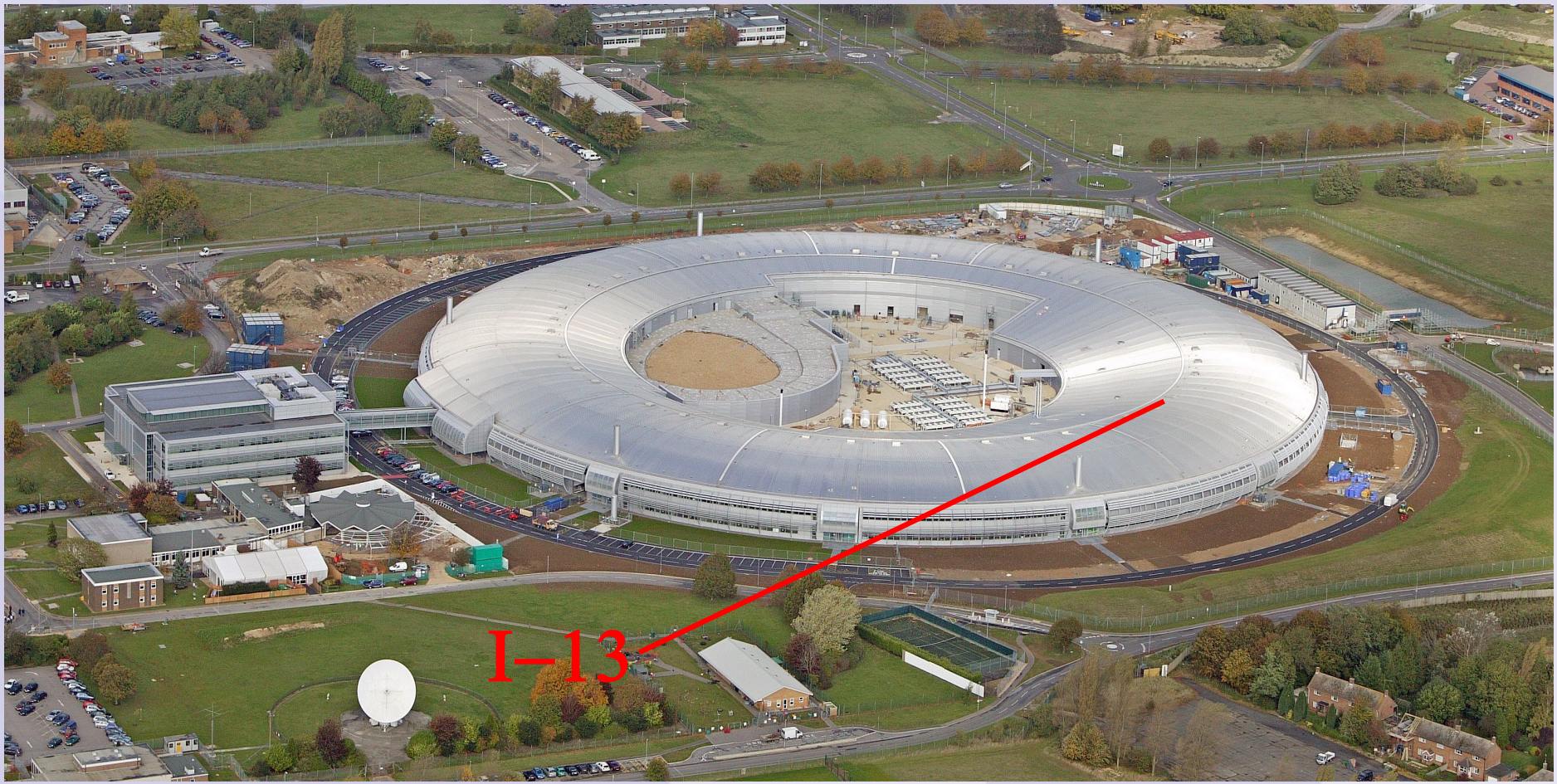

diamond

“First Light” - May 2006

ramped to 3GeV – Sept 2006

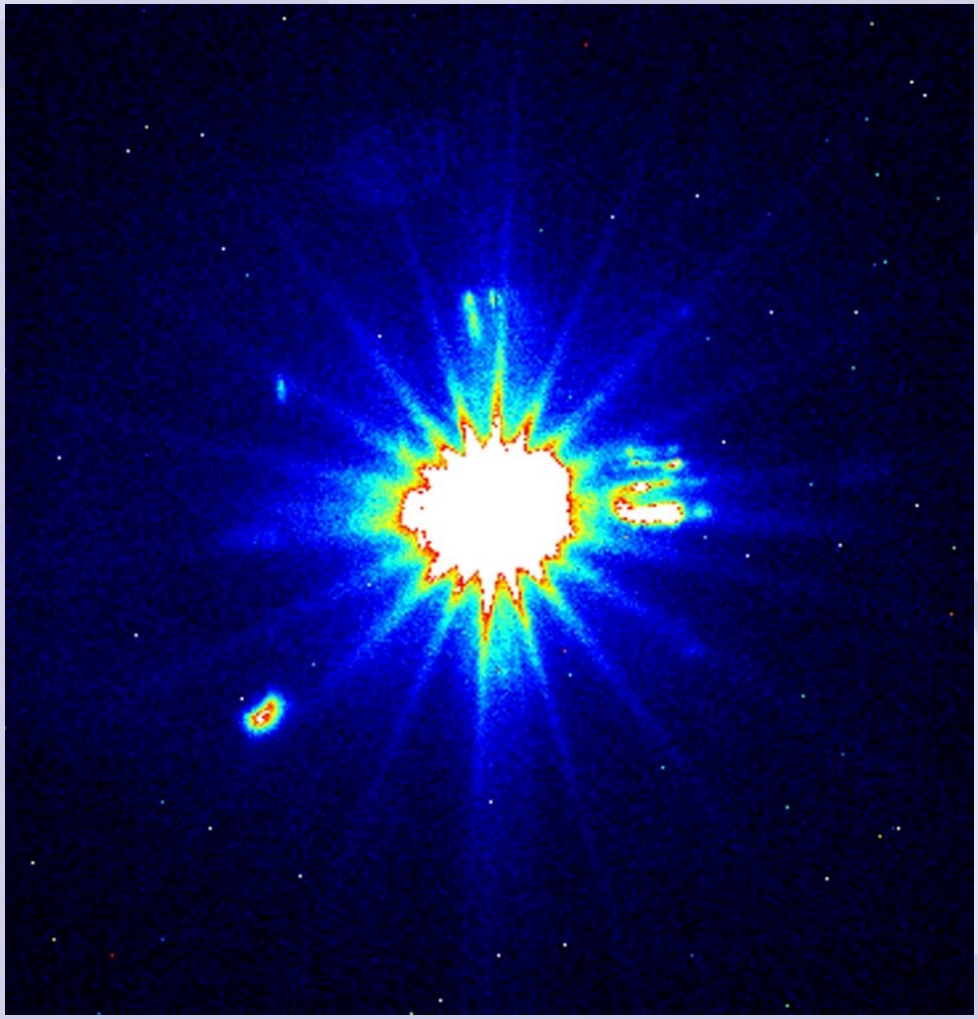

diamond

X-ray Undulator Principle

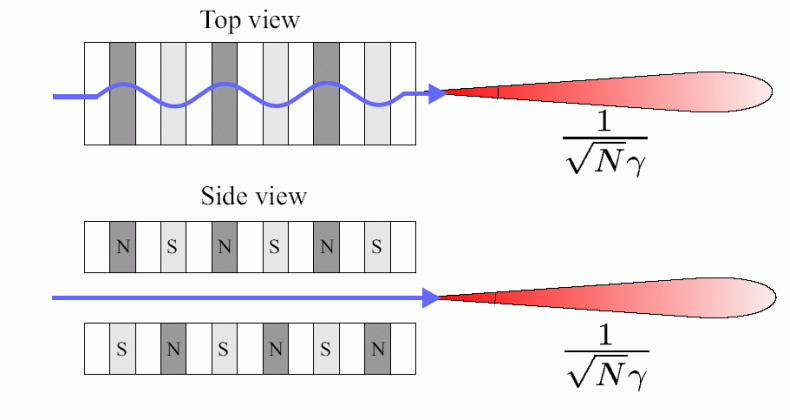

$$\lambda_X = \frac{\lambda_U}{2\gamma^2}\left\{1 + \frac{K^2}{2} + (\gamma\theta)^2\right\}$$

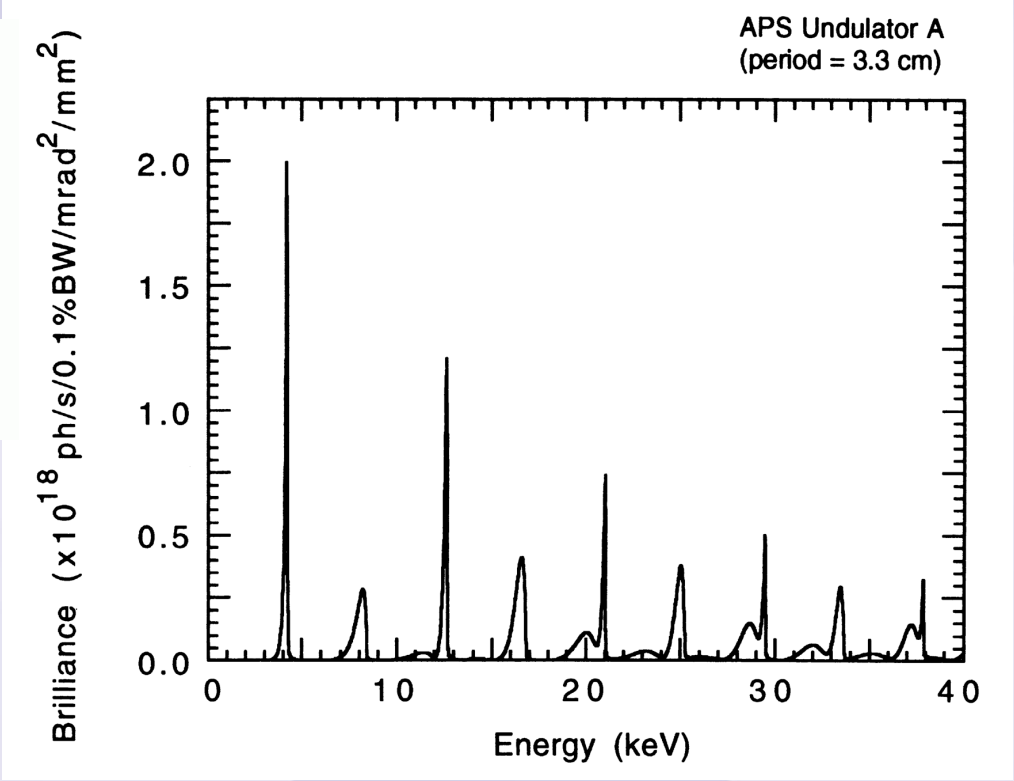

diamond

T ull-Field Mi

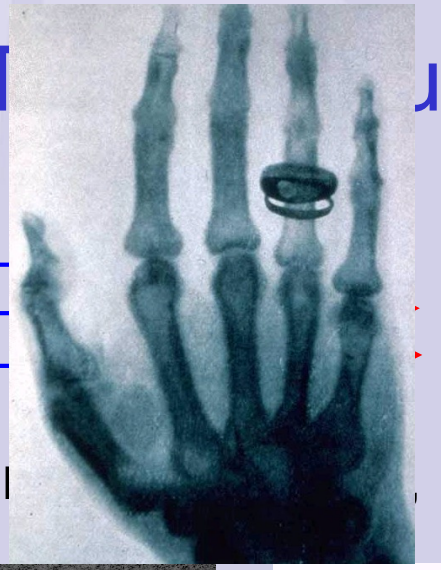

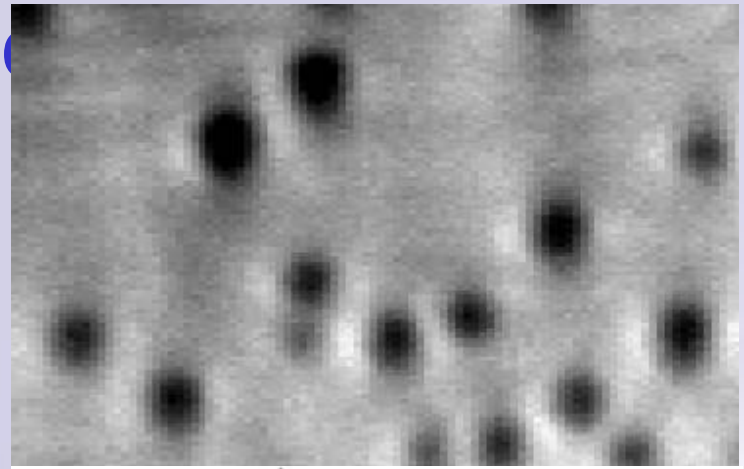

Coherent

Miao et al (1999)

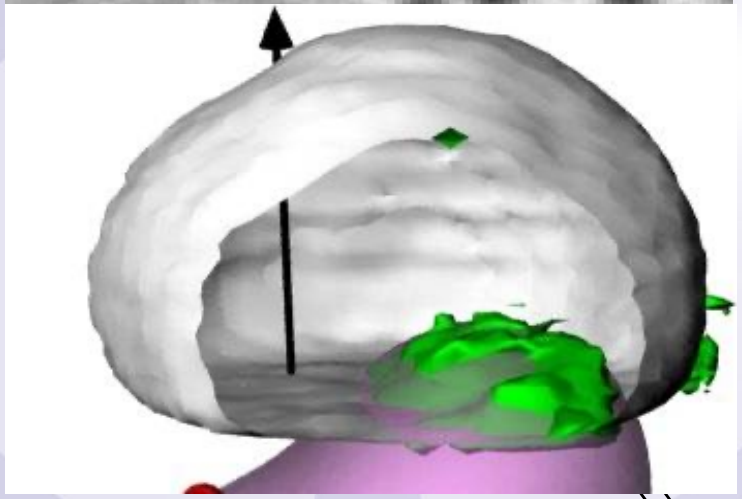

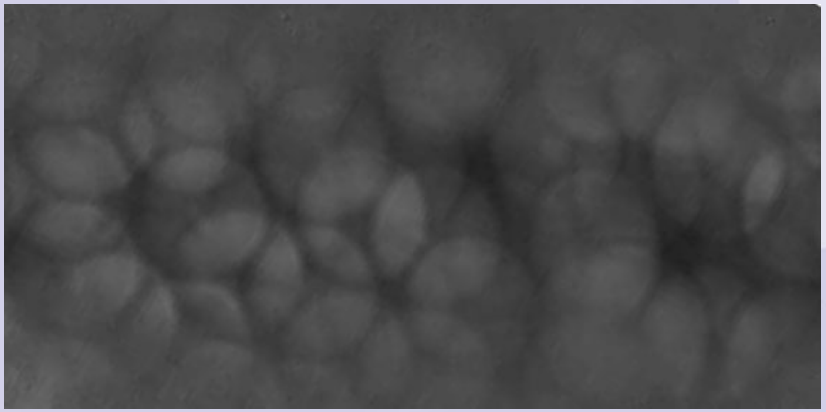

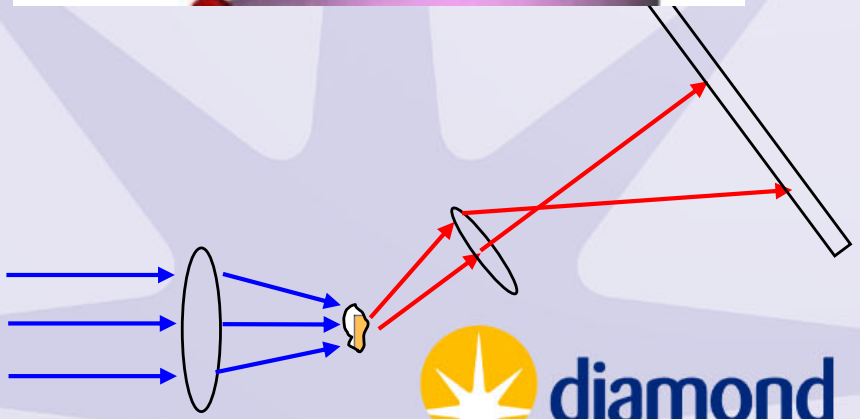

diamond

Full-Field Diffraction Microscopy

Fuel spray imaging

Argonne Center for Transportation Research (CTR)

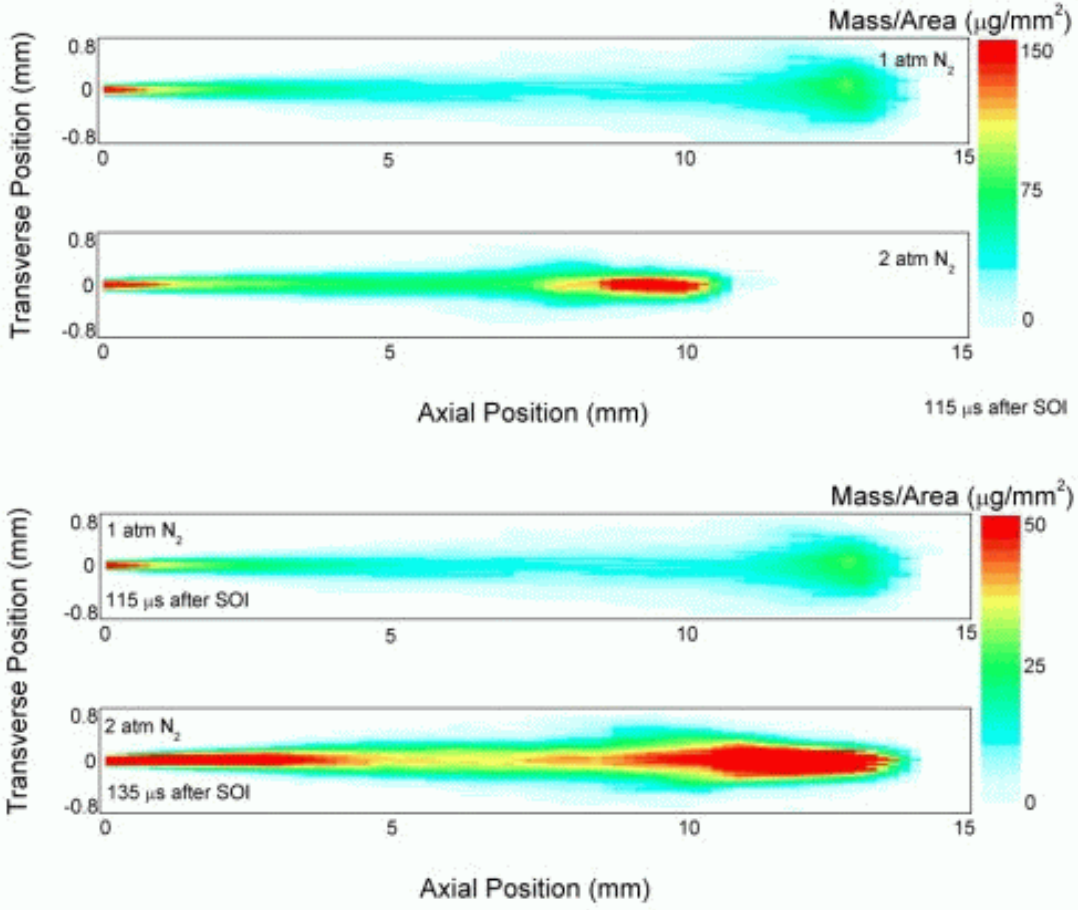

X-ray images of diesel fuel sprays encountering (top) atmospheric pressure and (bottom) two atmospheres of pressure. The measurements were taken 115 microseconds after the start of injection. Measured fuel density is indicated by color. The images show greater penetration at lower pressure and higher density in the higher-pressure case.

diamond

Grain boundaries in Al-Sn alloys

C. E. Krill, K. Döbrich, D. Michels, et al., Proc. SPIE Vol. 4503 (2002), 205-212

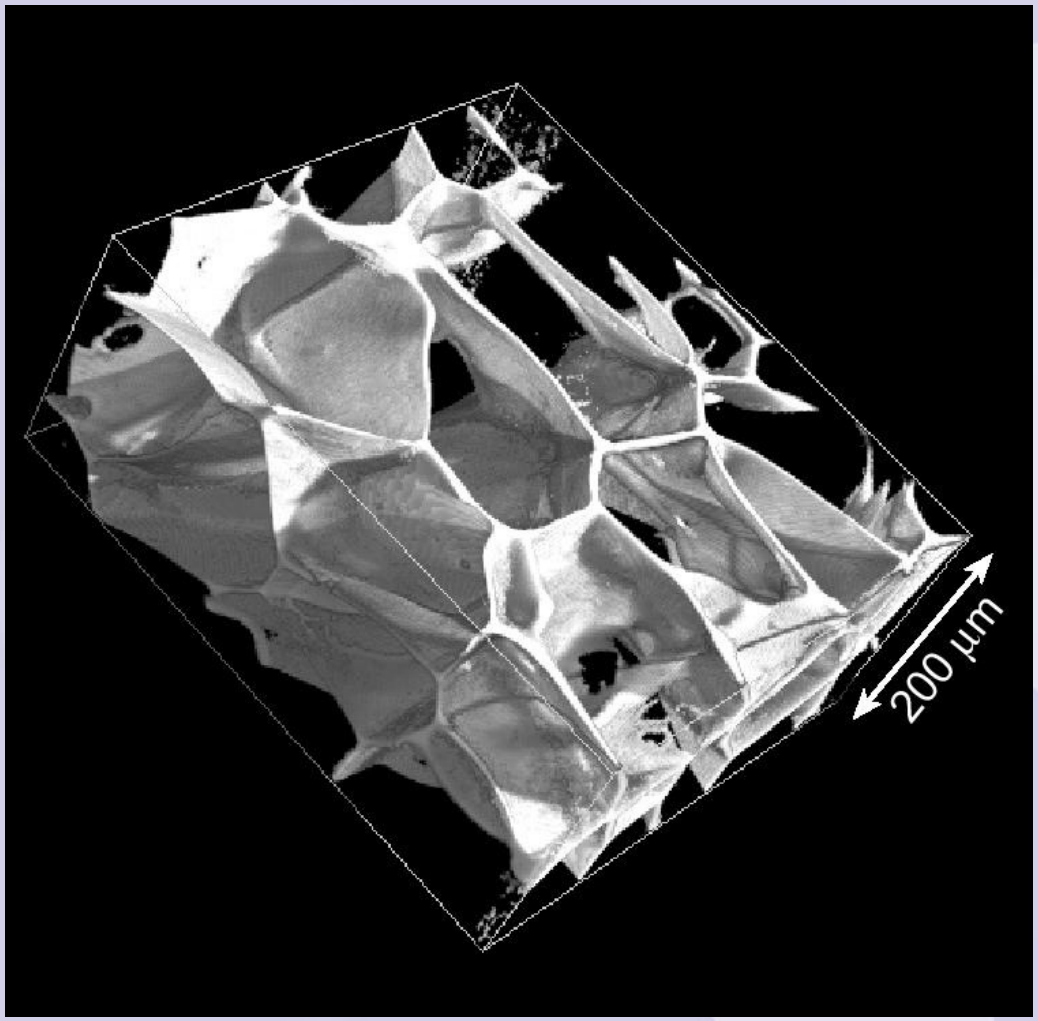

Christoph Rau
(ESRF)
now I-13 PBS

diamond

Injectable bone substitute (IBS) Enhancement of bone growth

P. Weiss, O. Gauthier, L. Obadia, et al., Biomaterials, Vol. 24(25), 4591-4601, 2003

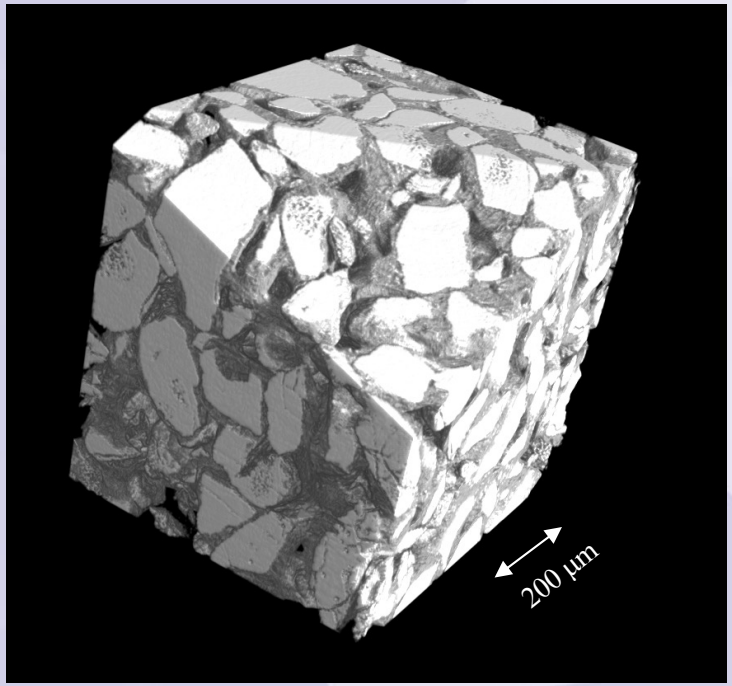

Christoph Rau
(ESRF)
now I-13 PBS

diamond

Application: Advanced IC Device

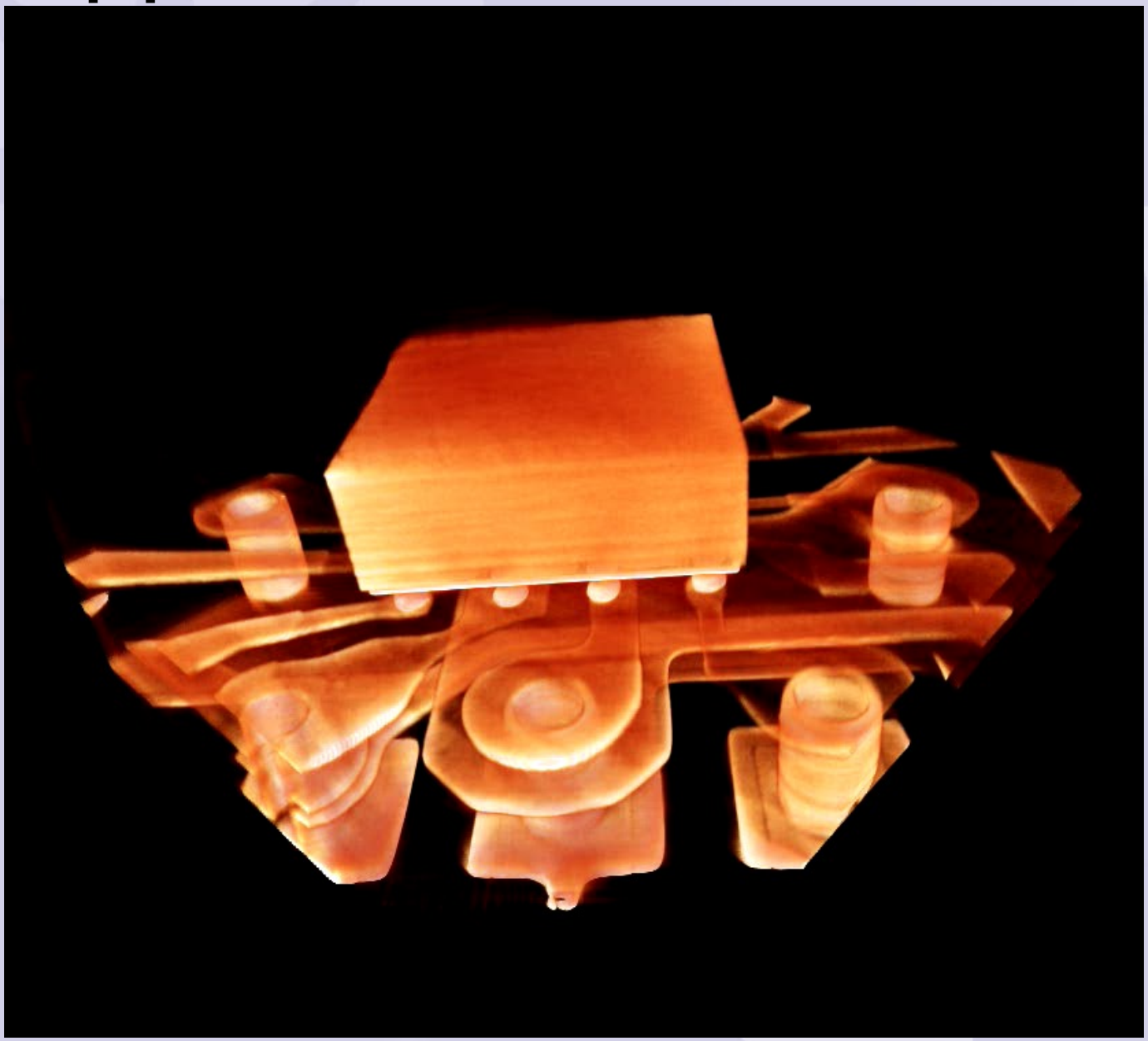

“nanoXCT”: Xradia commercial product

(Dr Wenbing Yun, CEO)

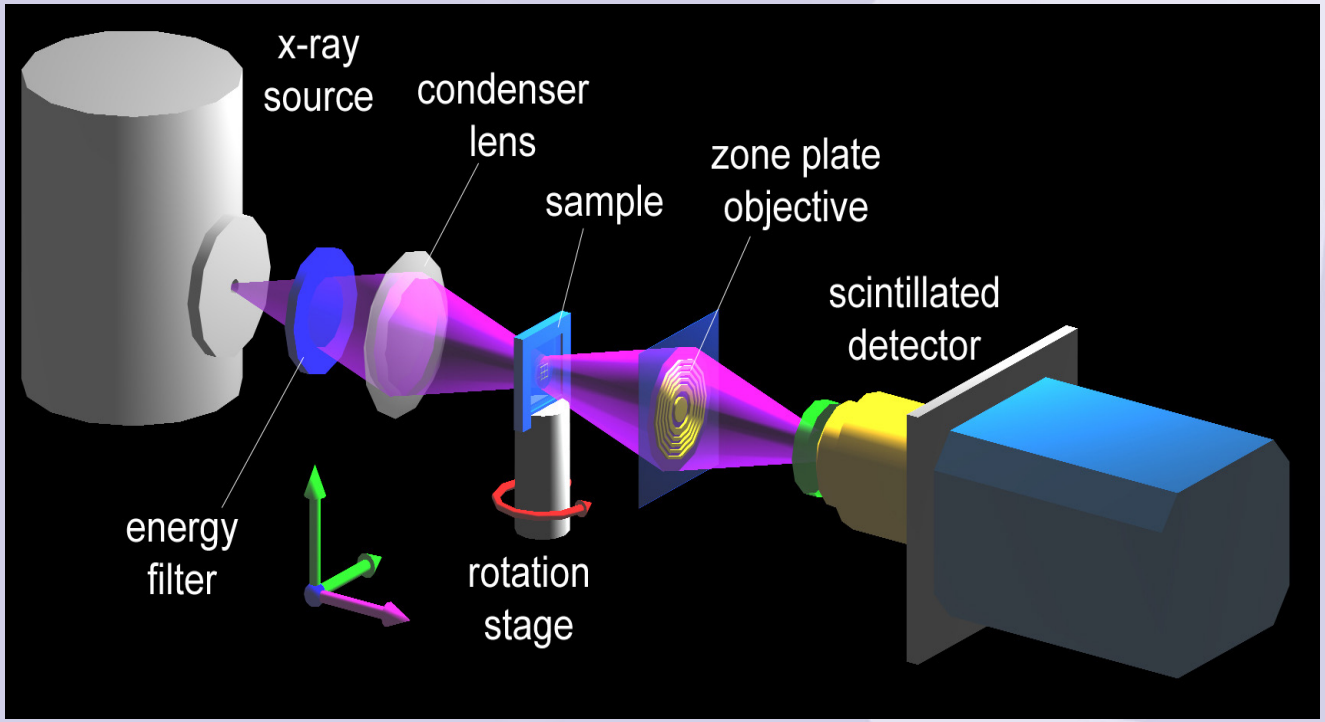

X-ray Zone-plate Lens

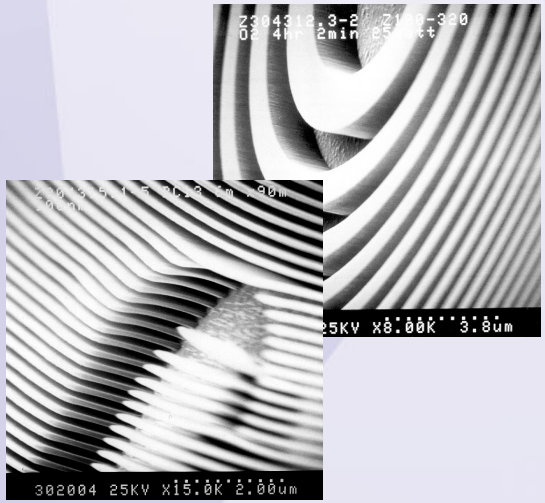

X-ray Tomography of Cu interconnects in IC Chip

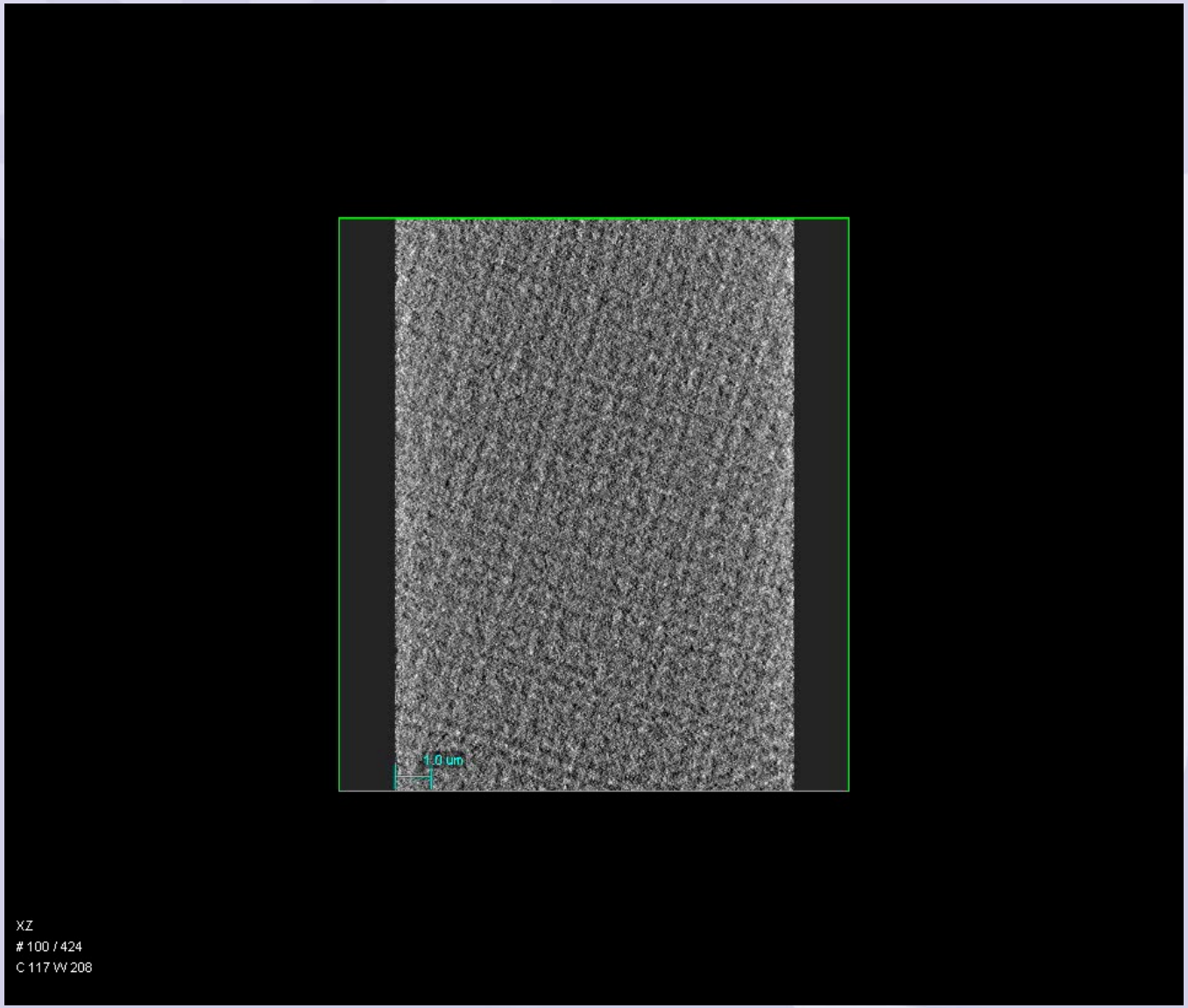

- 35nm imaging zone plate optic
- Cu (8 keV) Laboratory x-ray source
- Zernike Phase contrast Imaging

diamond

3D Imaging of Photonic Crystal

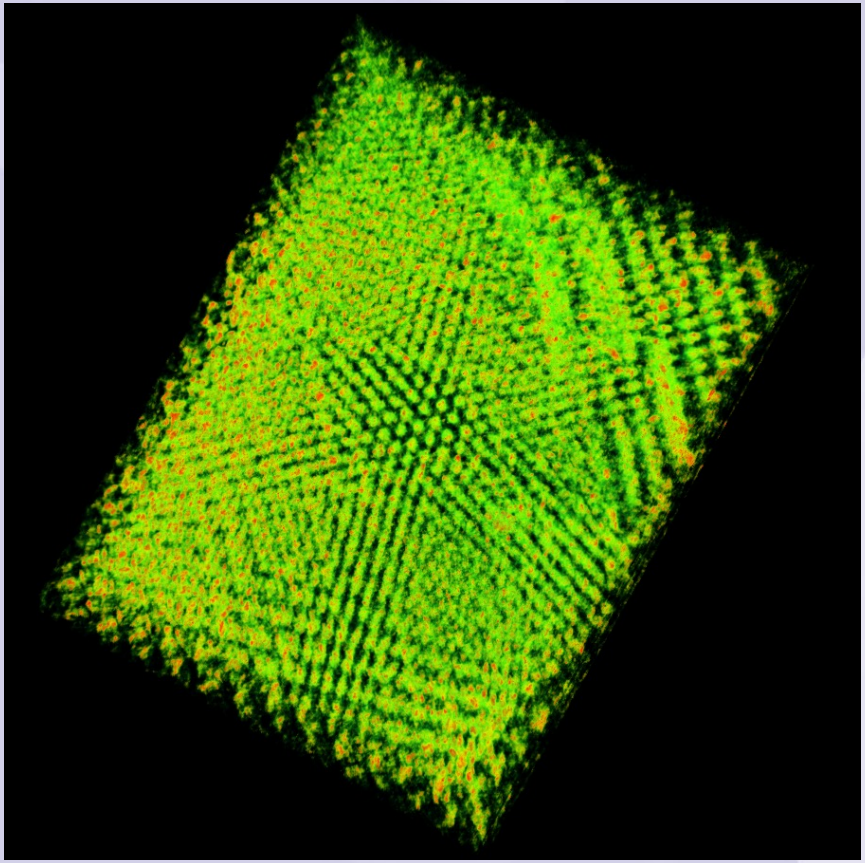

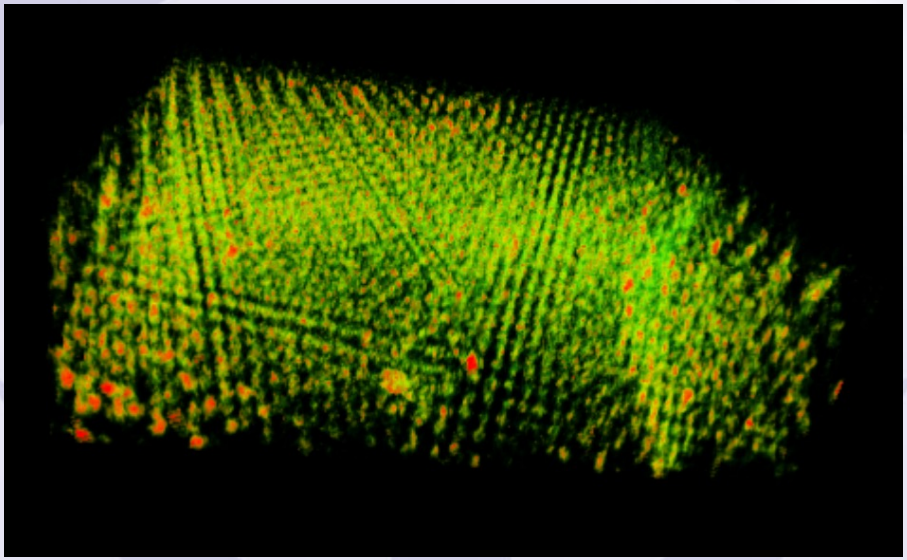

- Volume-rendering provides 3-dimensional perspective of the sample structure.

diamond

Grating results at ESRF ID19

T. Weitkamp , F. Pfeiffer, C. David, PSI

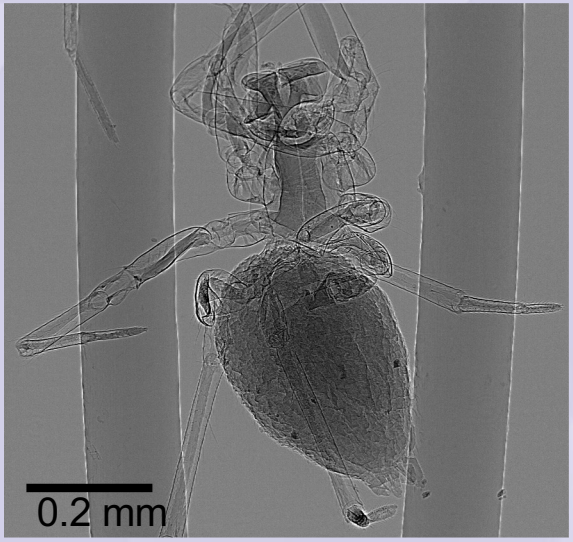

Transmission

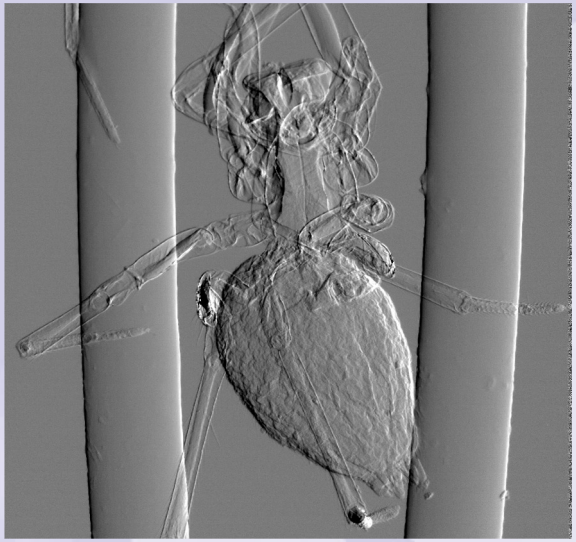

Phase gradient

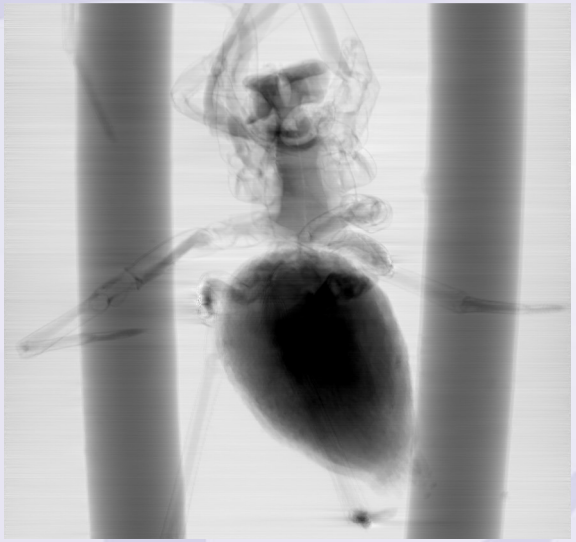

Phase

200 μm

diamond

Advanced Focusing Optics: Pathway for 5 nm Focusing of Hard X-rays (Q. Shen)

Multilayer Laue Lens

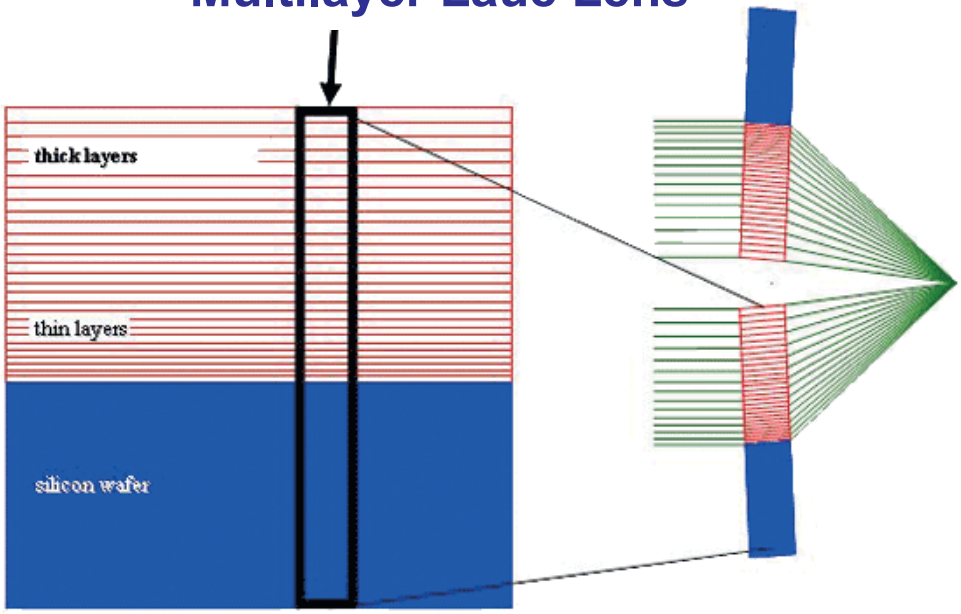

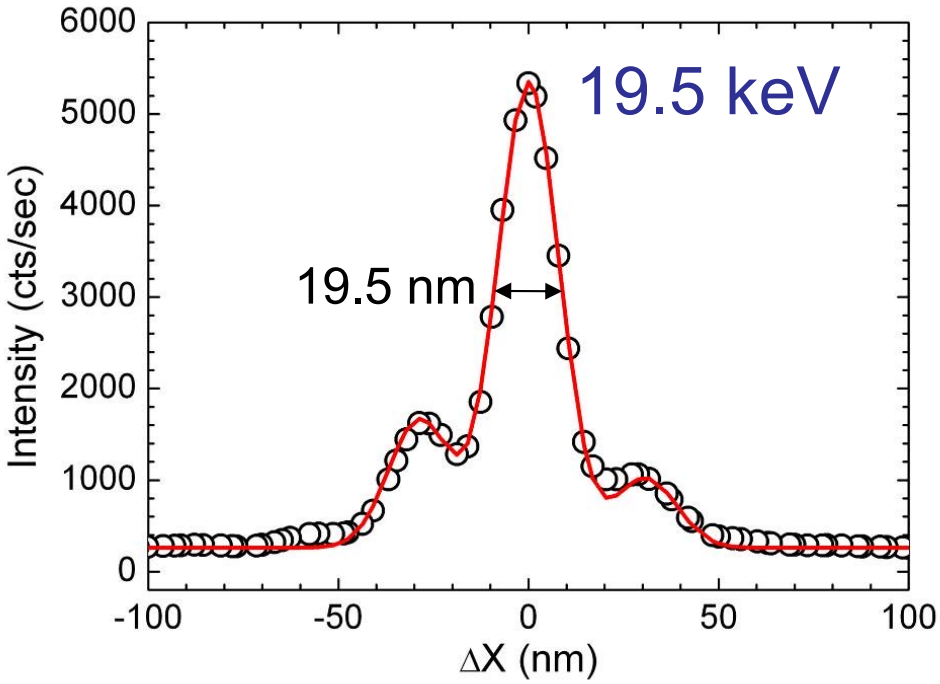

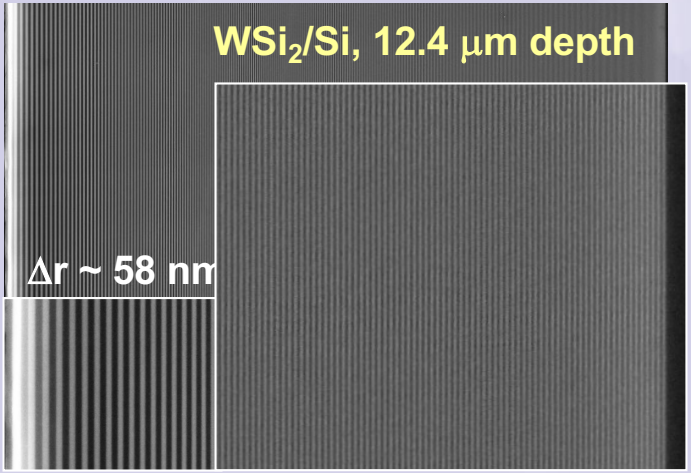

H.C. Kang, J. Maser, G.B. Stephenson, C. Liu, R. Conley, A.T. Macrander, S. Vogt *Phys. Rev. Lett. 96, 127401 (2006)*

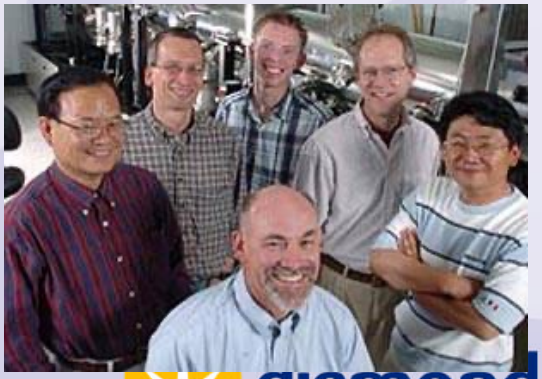

diamond

Phase-Contrast X-ray Diffraction Microscopy

*P. Fenter, C. Park, Z. Zhang, and S. Wang, in review (2006)

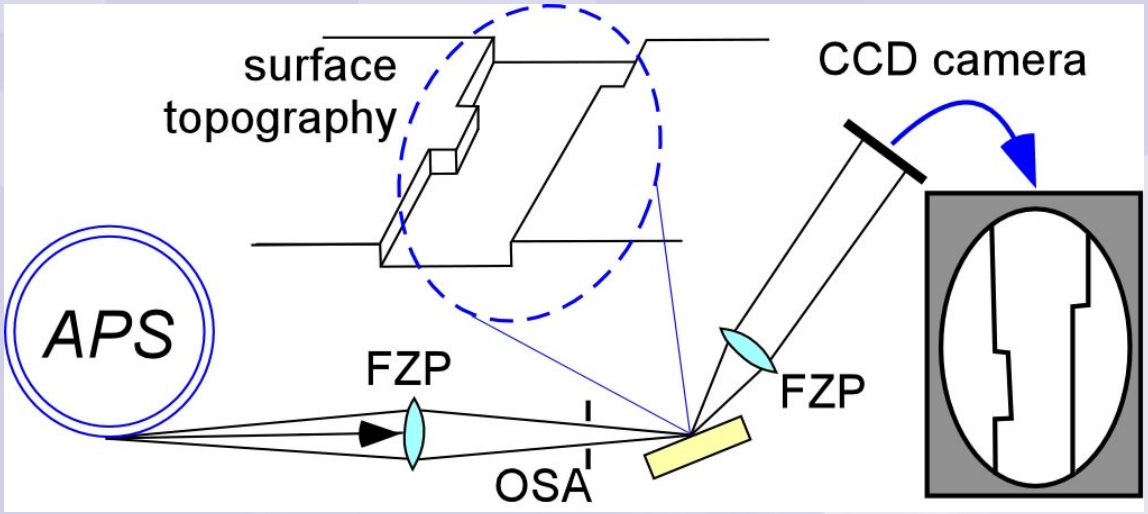

Intensity contrast at CTR:

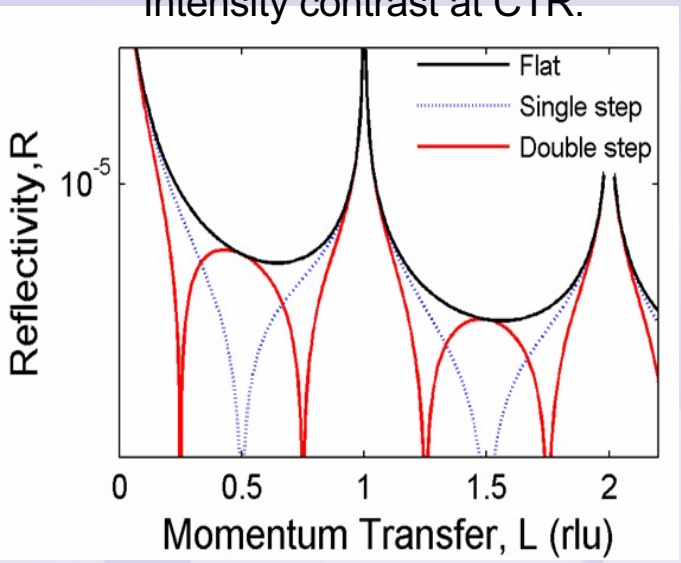

Phase contrast mechanism:

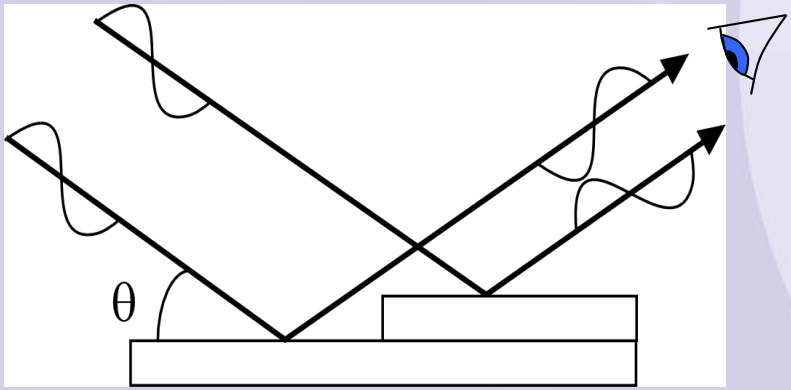

X-ray Reflection Interface Microscopy

Characteristics:

→ Strong contrast at defects (~100%), but weak reflected beam intensity ($R < 10^{-5}$)

→ Sub-nm vertical sensitivity, but modest lateral resolution (~100 nm, set by FZP)

diamond

Observation of Surface Step Distributions

P. Fenter, C. Park, Z. Zhang, and S. Wang, in review (2006)

APS 12-ID-D, December, 2005

Step distributions on Orthoclase, $KAlSi_3O_8$ (001)

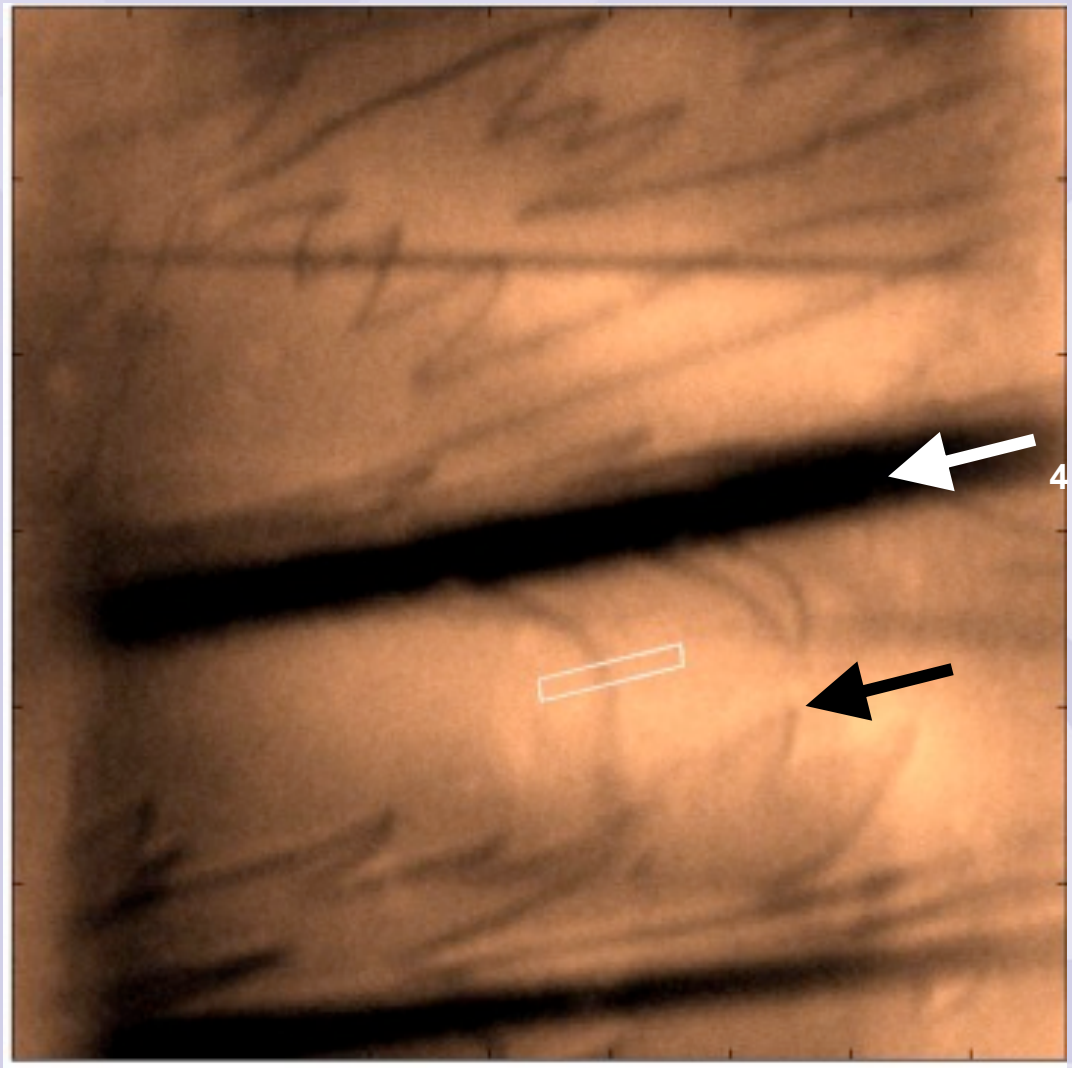

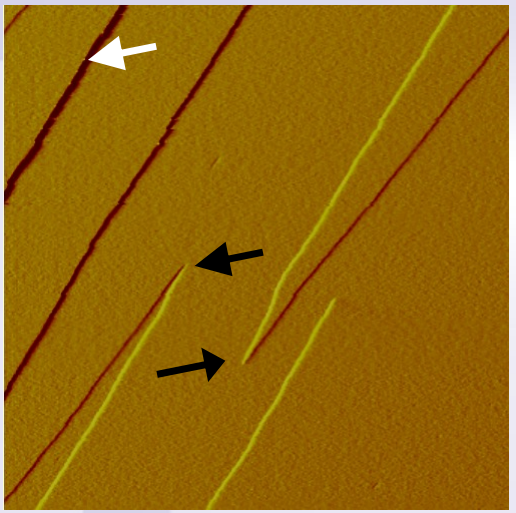

Teng et al., GCA **65,** 3459 (2001)

Imaging Conditions:

- θ = 1.4°
- E = 10 keV
- L = 0.25 rlu (Q = 0.24 Å^{-1})
- Sample held in air

diamond

Angular rheology and diffraction

Diffraction – typically used to study structure

- also sensitive to position and orientation

Angular rheology techniques:

- tagging
- asymmetric particles

Diffraction does not require such sample preparation

- sensitive to lattice planes
- penetrate various media – opaque
- embedded/coated particles
- angular resolution suitable for Brownian motion studies

diamond

Diffraction for Angular Rheology

- Each crystal which obeys the diffraction condition on powder ring
- Two orthogonal rotations can be observed

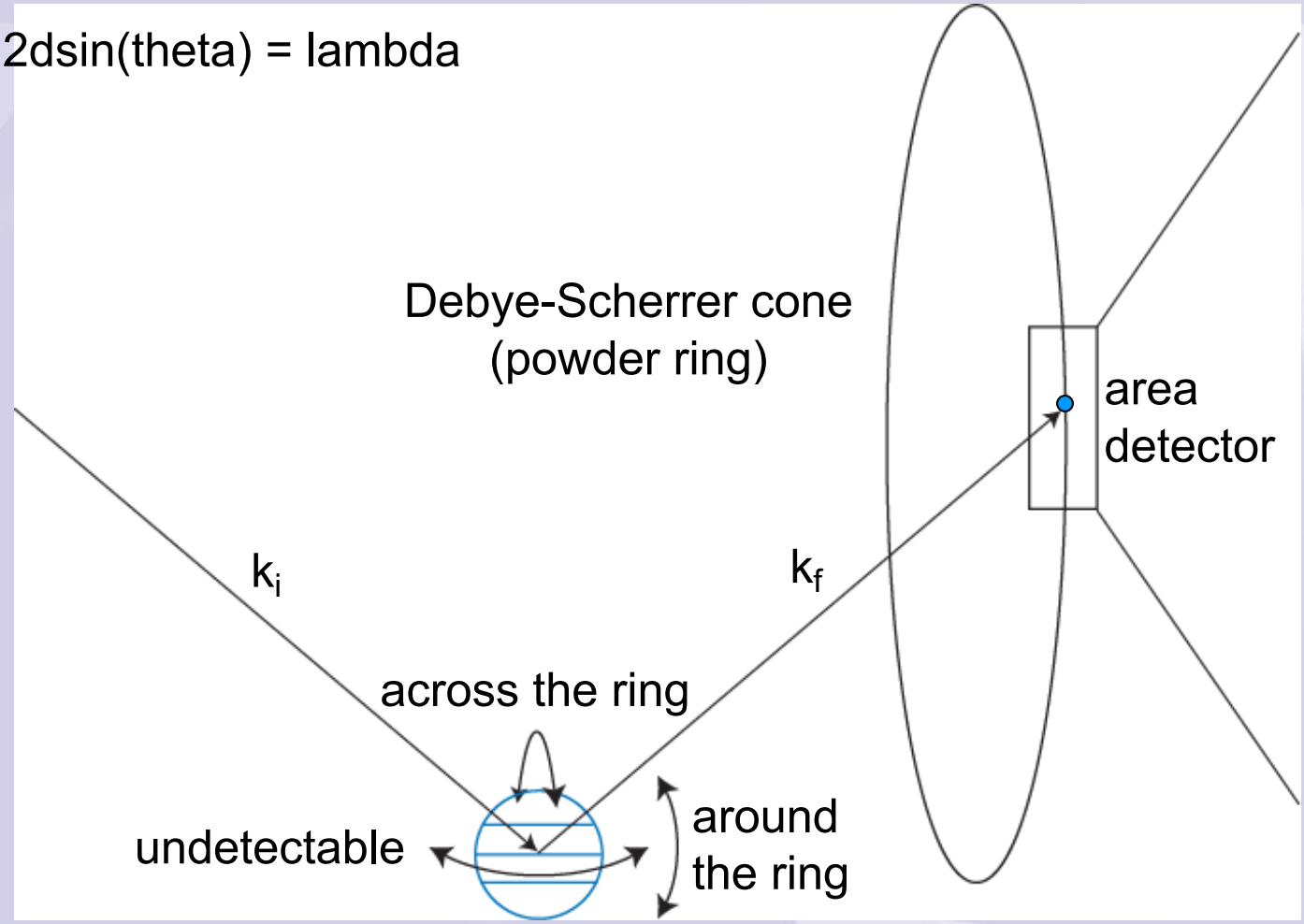

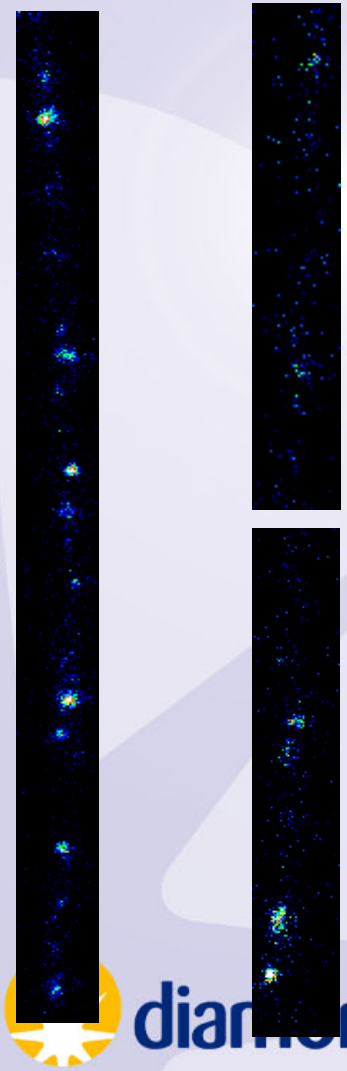

Experimental Setup

beamline 34-ID-C at Argonne

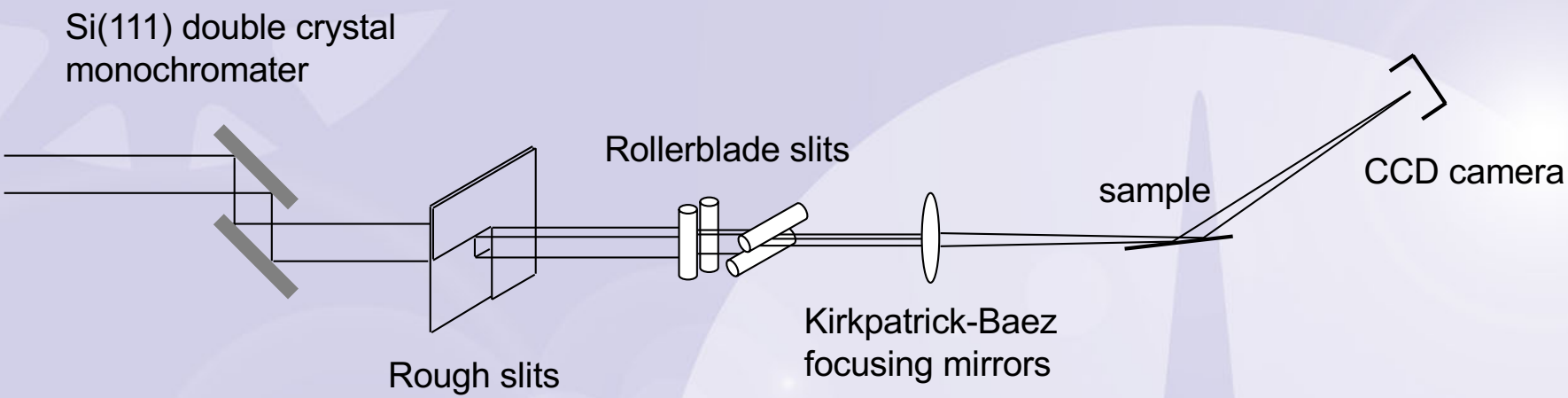

- Paint:TiO_2 pigment, surfactant, polymer, solvent
- Model system: alumina, fatty acid, vary temperature
- thesis project of Meng Liang

diamond

Peak positions vs time: paint

integrate across ring (to isolate motion around the ring)

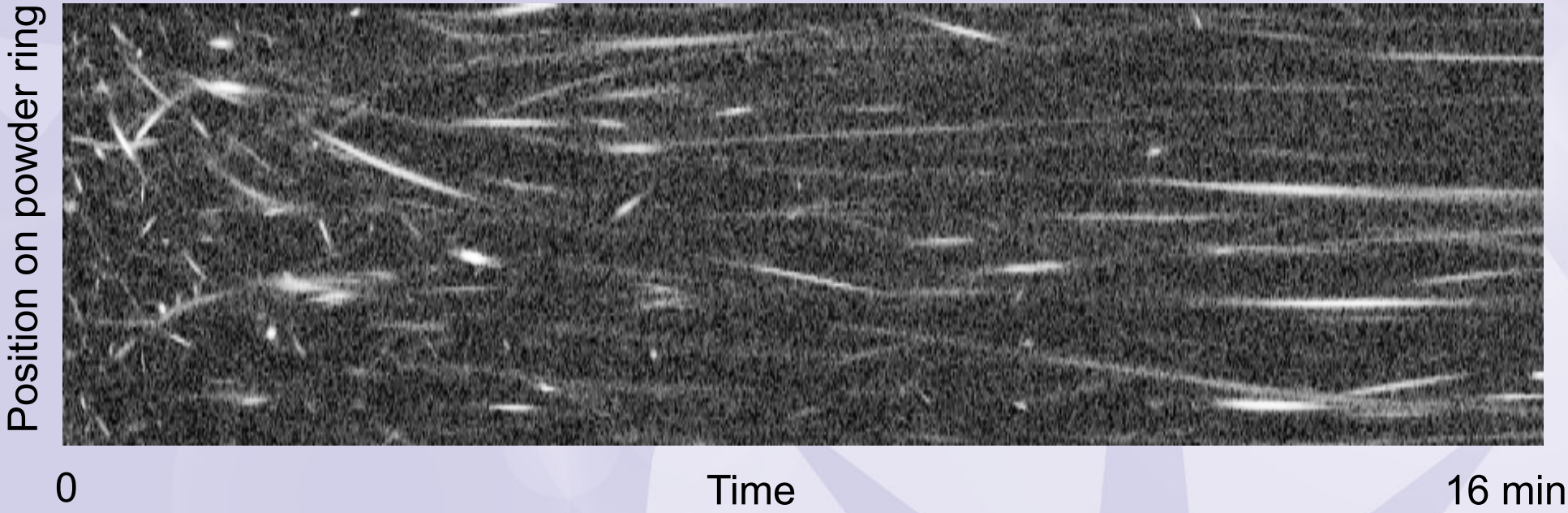

- Dry paint is still mobile
- Slowing down due to drying in the x-ray beam
- distribution of rotational velocities

diamond

Peak positions vs time: model

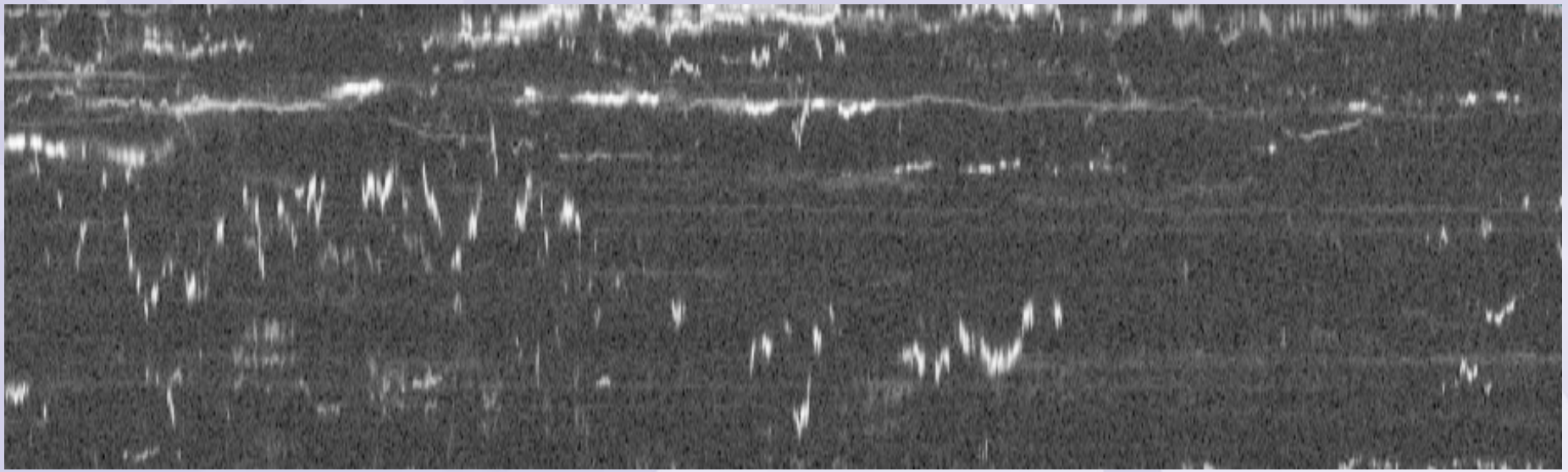

- Al_2O_3 in octanoic acid ($C_8H_{16}O_2$)
- Another type of motion – Brownian motion instead of rotational diffusion

diamond

Brown407-38

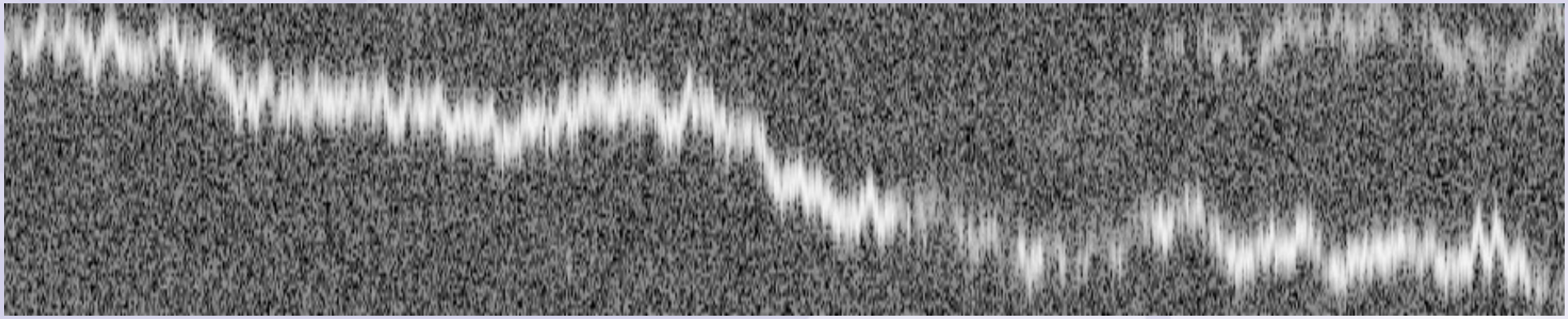

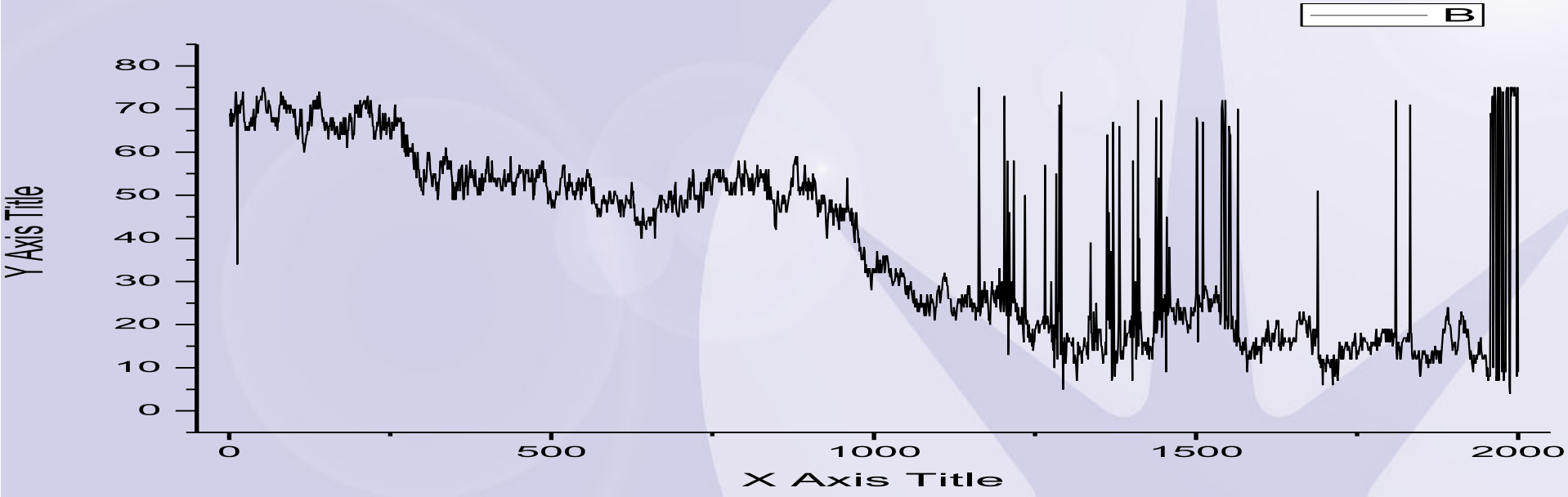

The results of the particle tracking – there are a few outliers, especially because of the particle coming in towards the end – truncate data (I can also write a program to only look for displacements within a range but that will take some more work)

Truncated data range : frames 14-1162

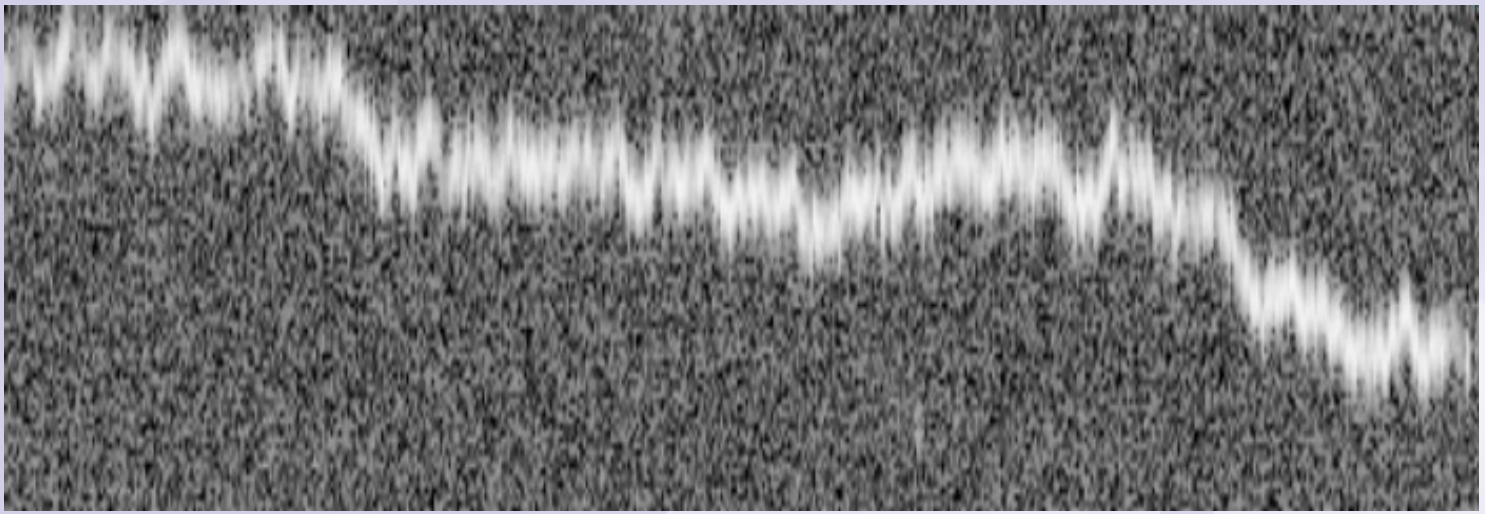

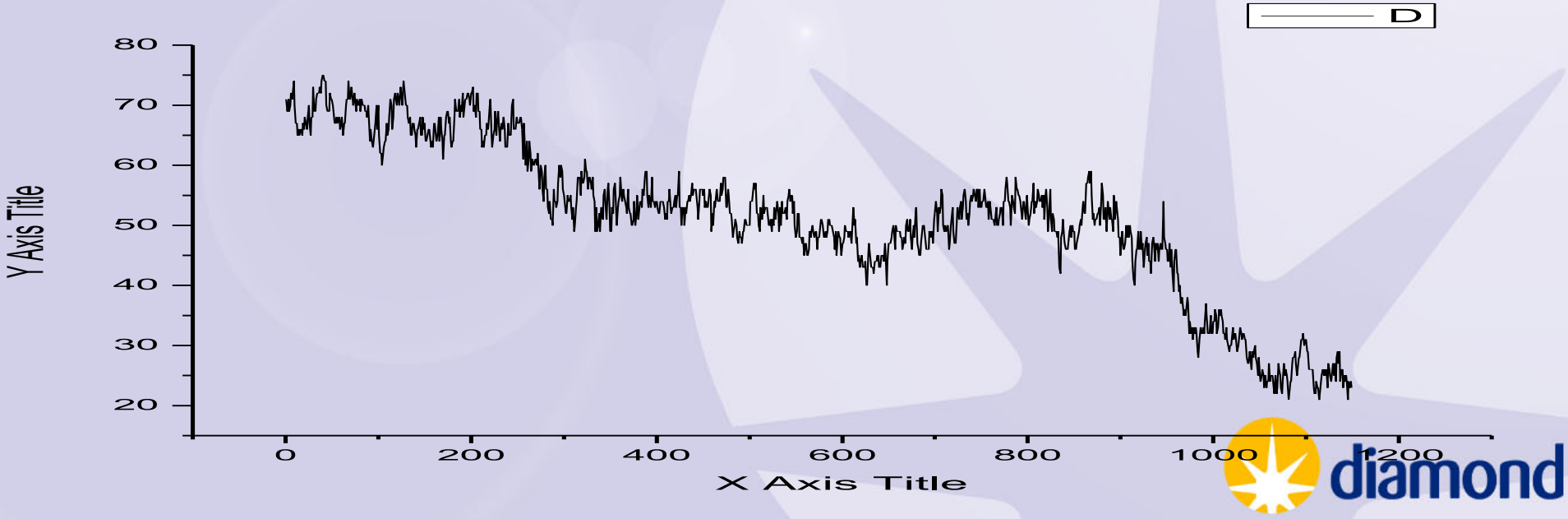

• Result of MSD vs frames/time - two different slopes (think it is due to large drop seen in the data towards the end)

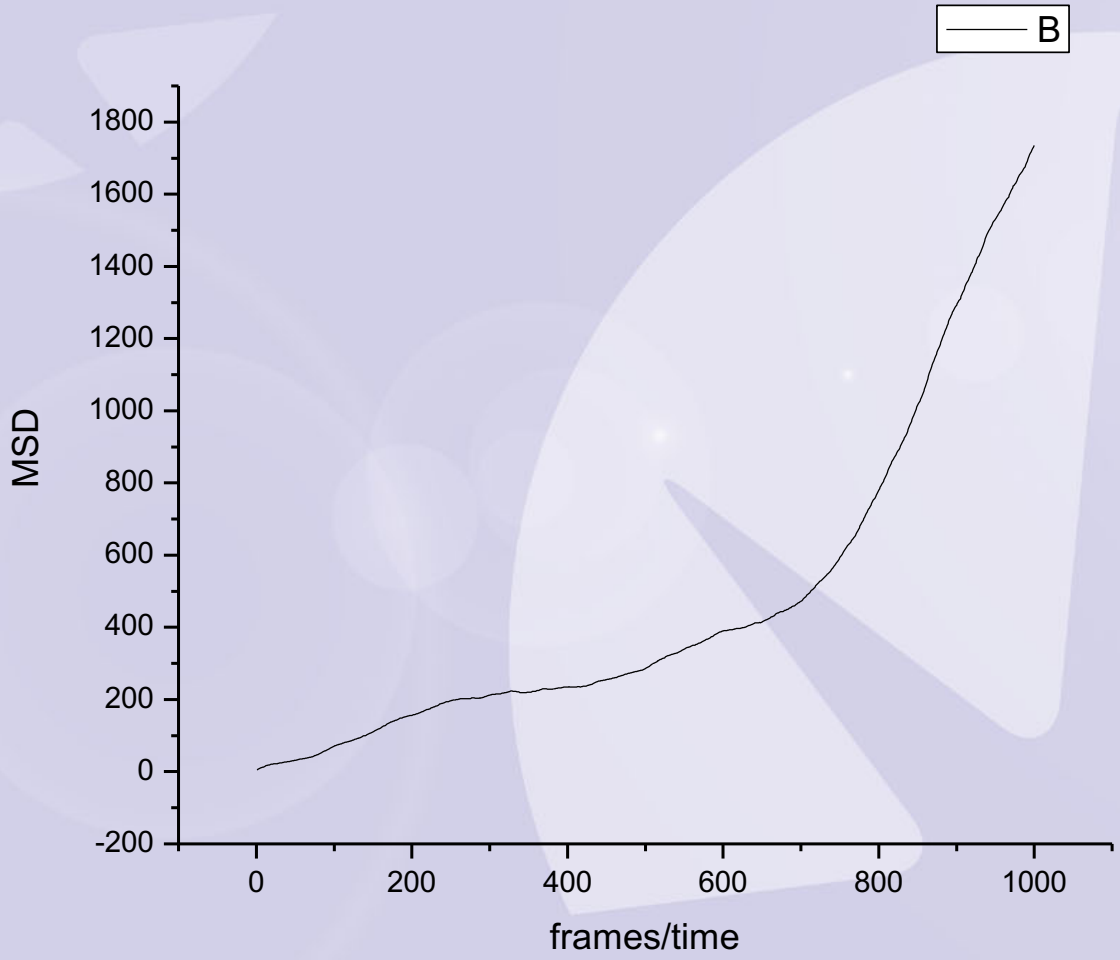

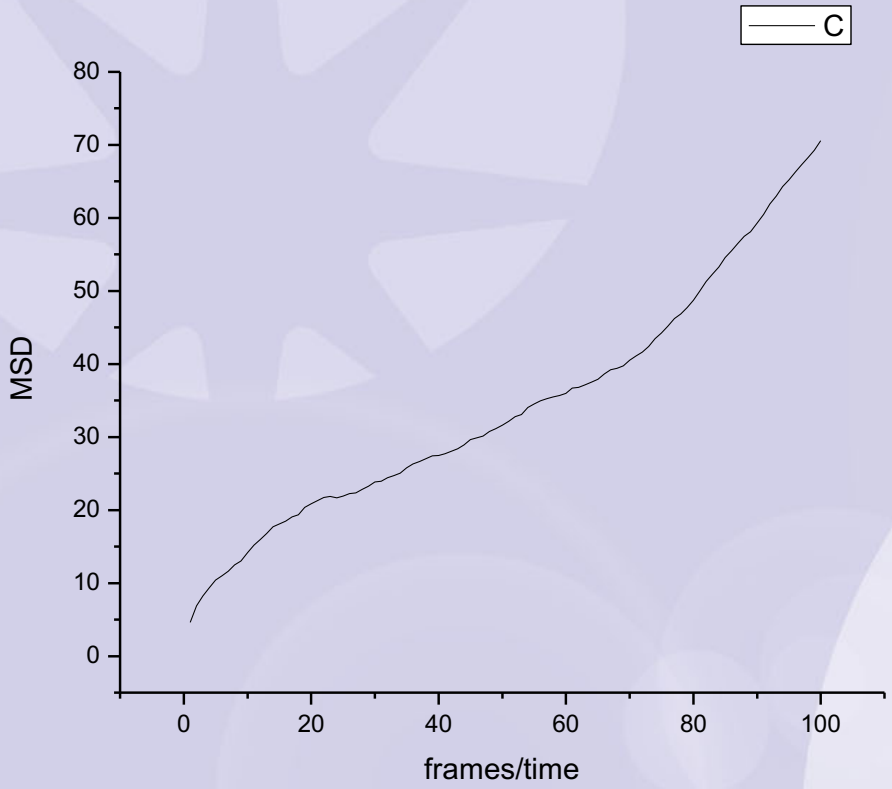

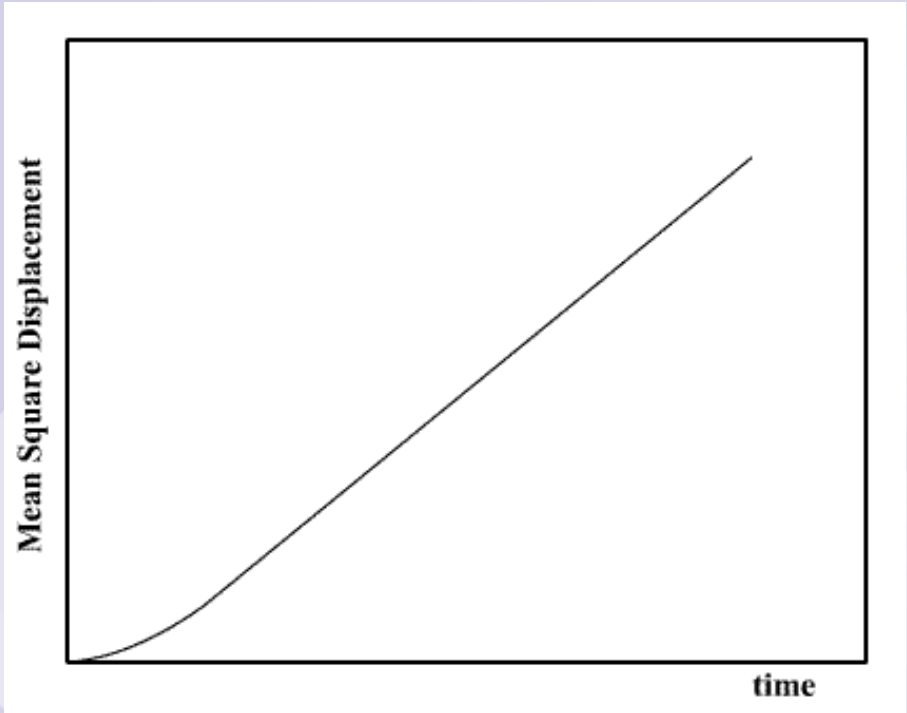

The lower part of this graph, between 0-70 looks similar to a brownian motion graph. The one on the right is a standard graph, where the particles start to have a MSD dependence on time after the first “collision”

Ref: http://www.compsoc.man.ac.uk/~lucky/Democritus/Theory/msd.html

diamond

Future work planned on paint

- X-ray diffraction allows us to see the rotational motion
- Pigment particles in dry paint are still rotationally mobile
- Paints undergo rotational diffusion
- Alumina particles in fatty acid show Brownian fluctuations

- Quantify rotational speeds and directions: particle tracking
- Look at motion across powder ring as well as along ring
- Time resolution is limited by detector read out time:
  faster detectors mean better time resolution
- How coatings and media affect the rotation

diamond

Size-dependent Melting of Au Particles

P. Buffat and J-P. Borel, Phys. Rev. A 2287-97 (1975)

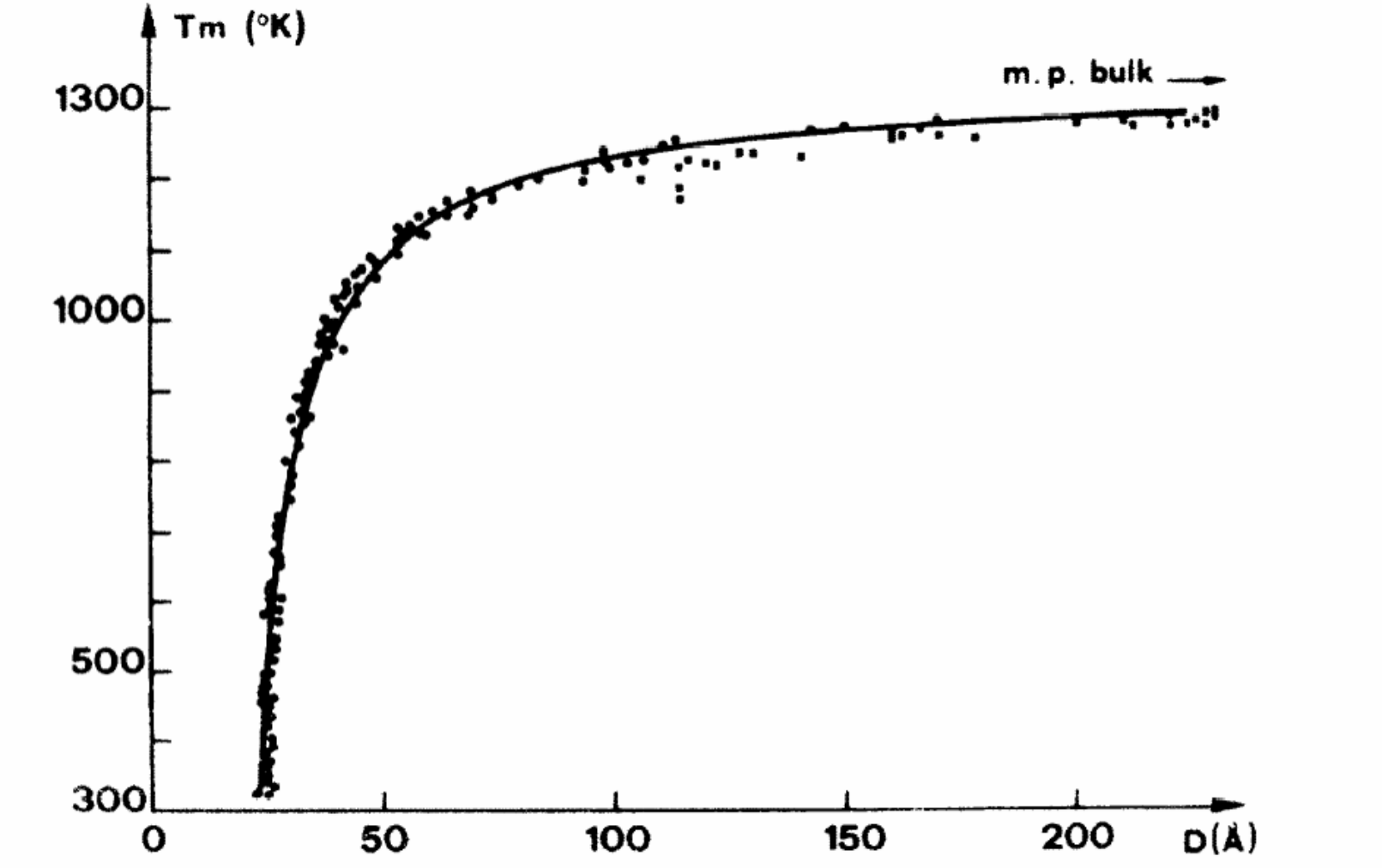

Lensless X-ray Microscope

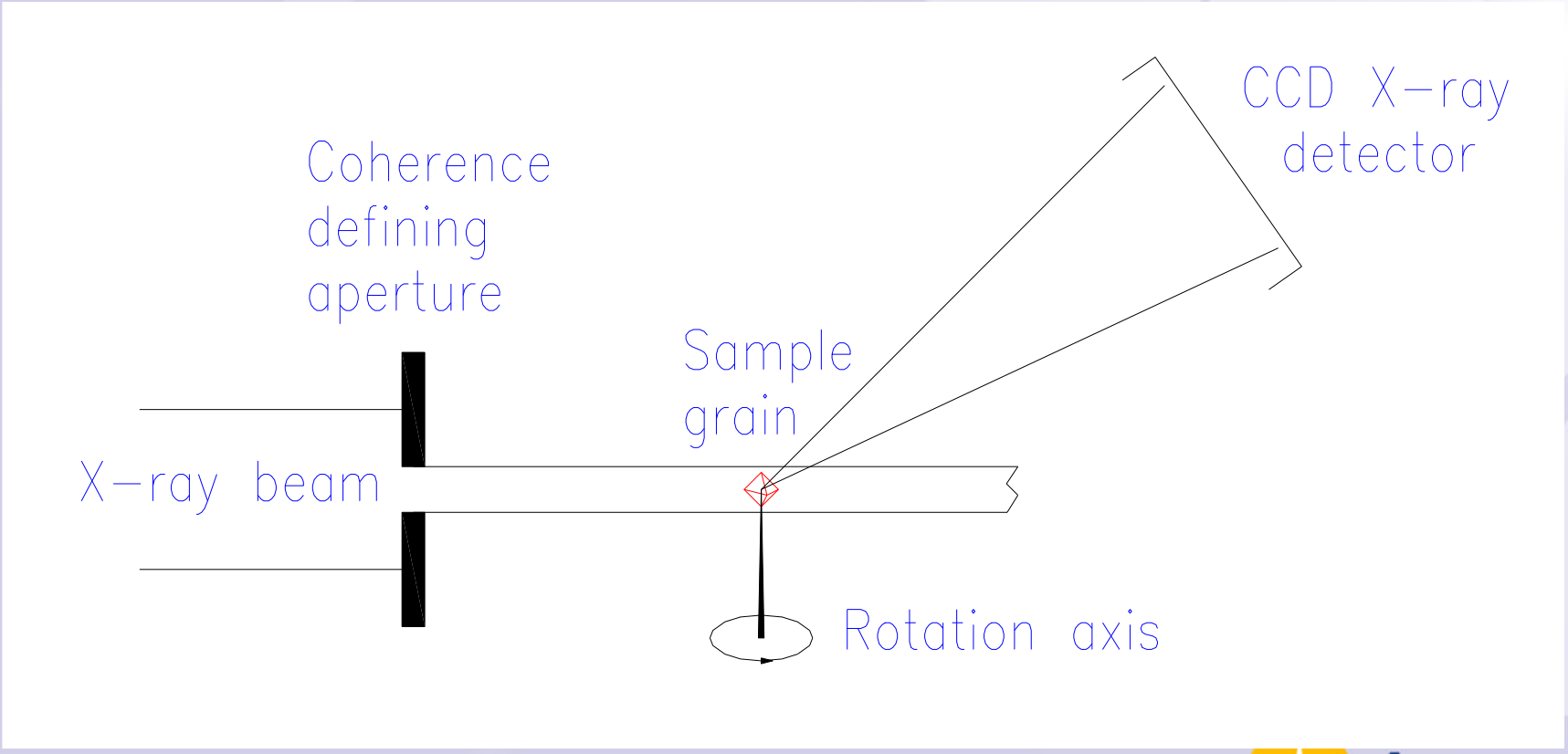

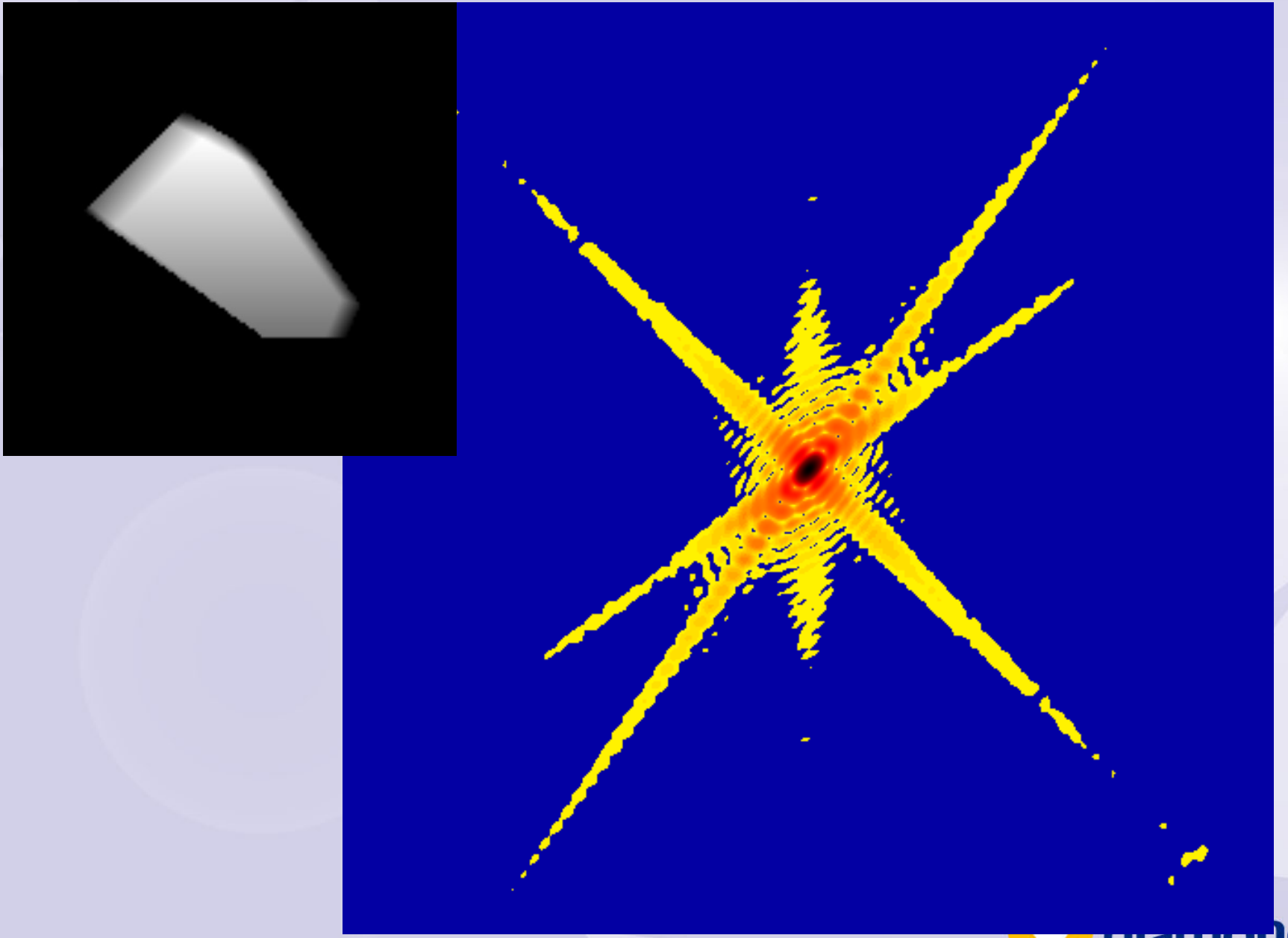

Reconstruction of Ag Nanocrystal

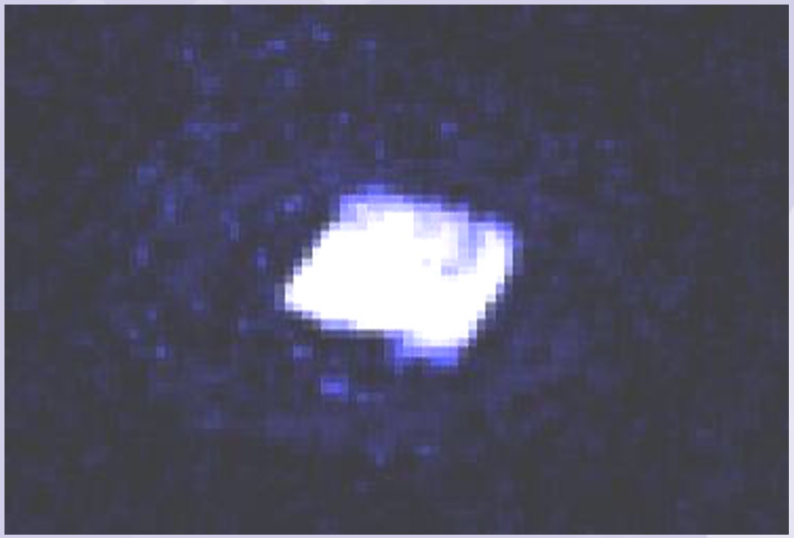

200nm

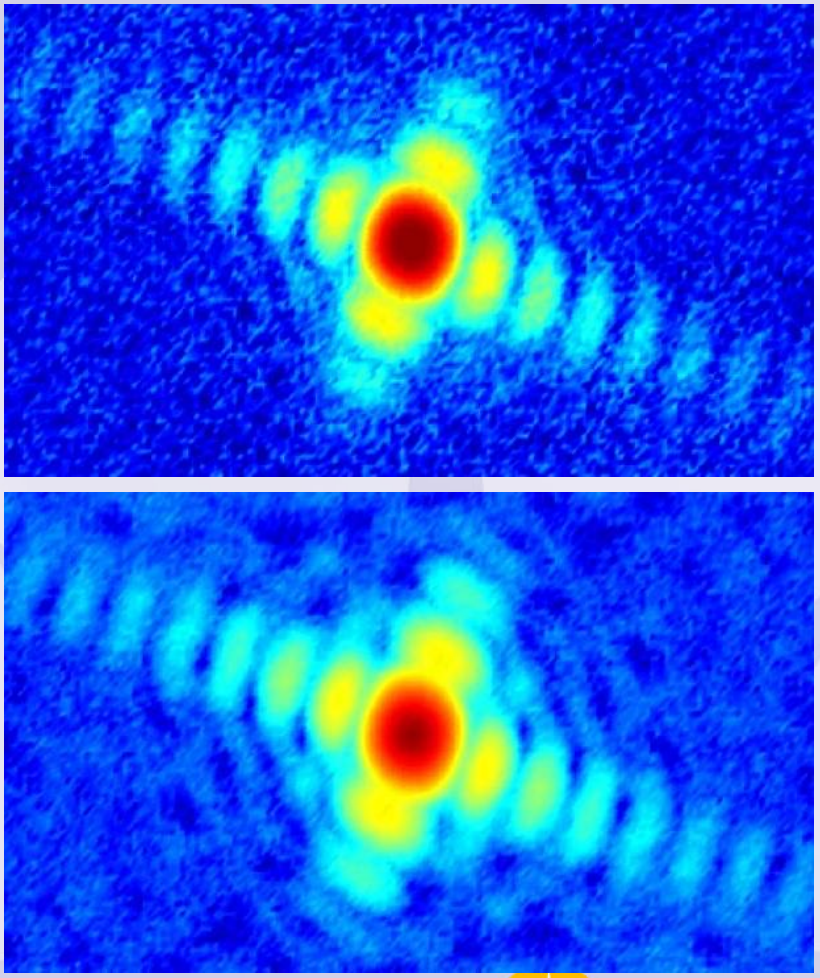

diamond

In situ growth of Pb crystals

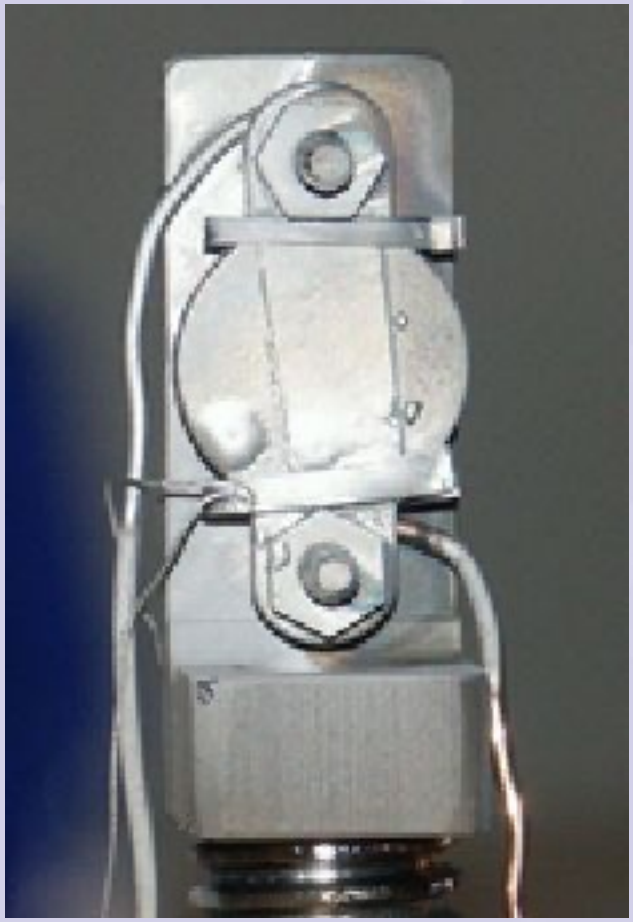

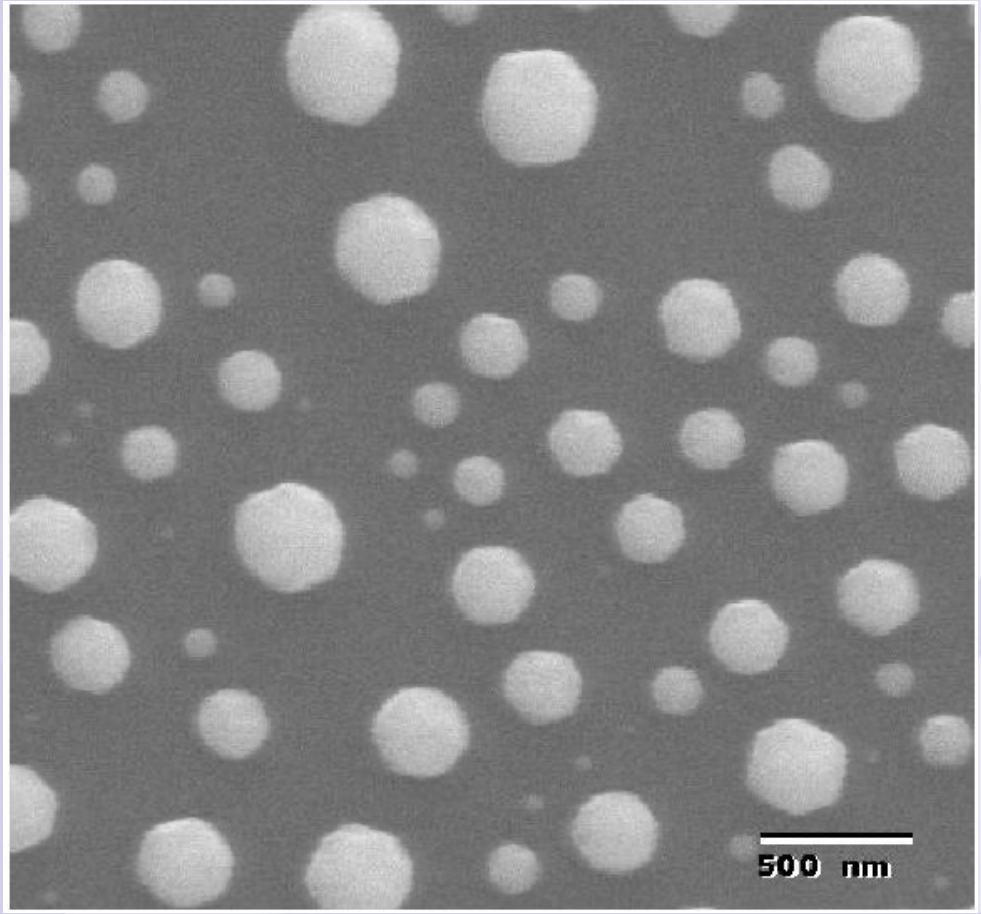

diamond

Coherent Diffraction from Crystals

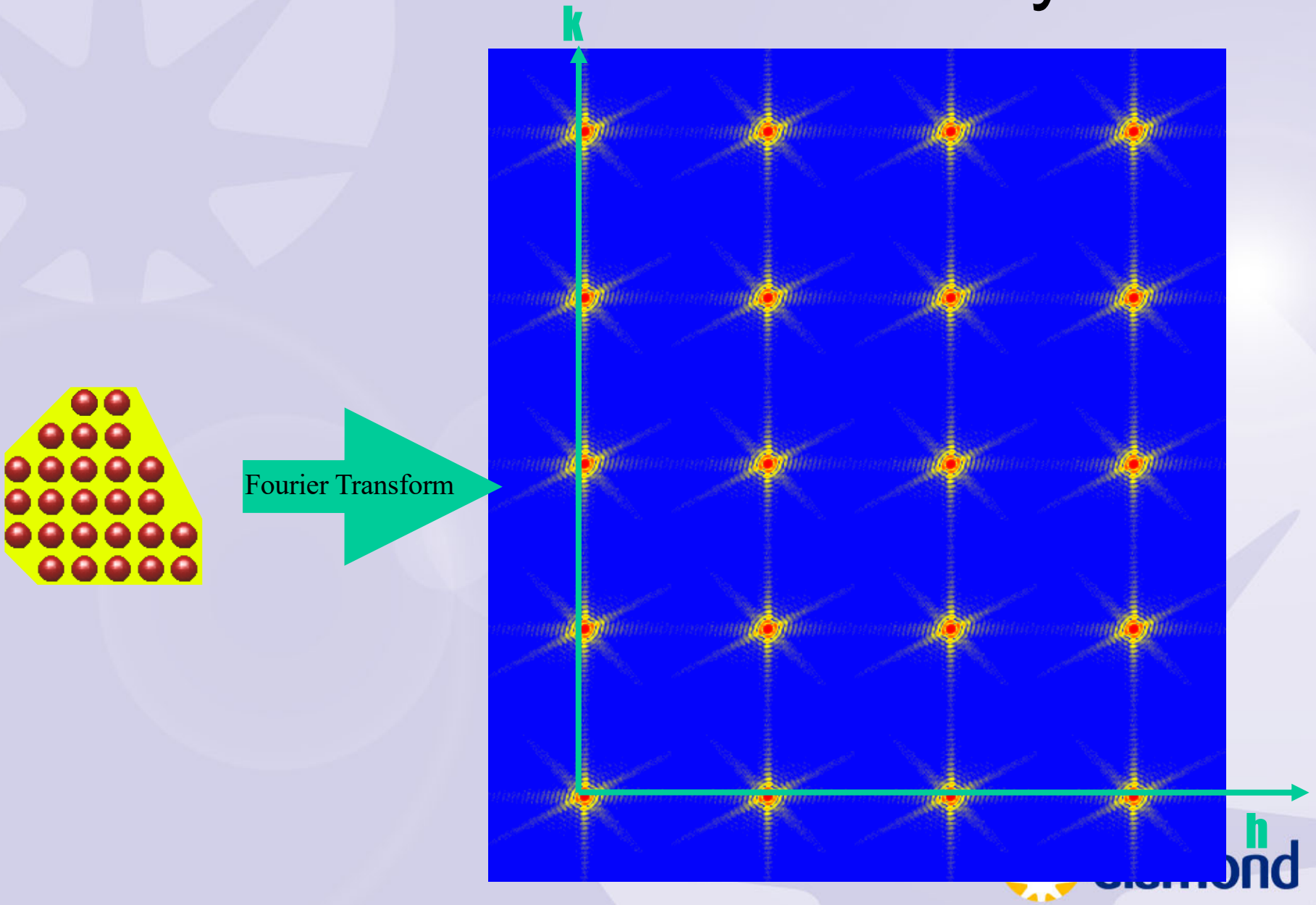

Diffraction by Strain of Point Defect

$$A \sim \sum e^{iQ\cdot(R_j+u_j)}$$
$$\approx \sum e^{iQ\cdot R_j}\,(1+iQ\cdot u_j)$$

Imaginary density

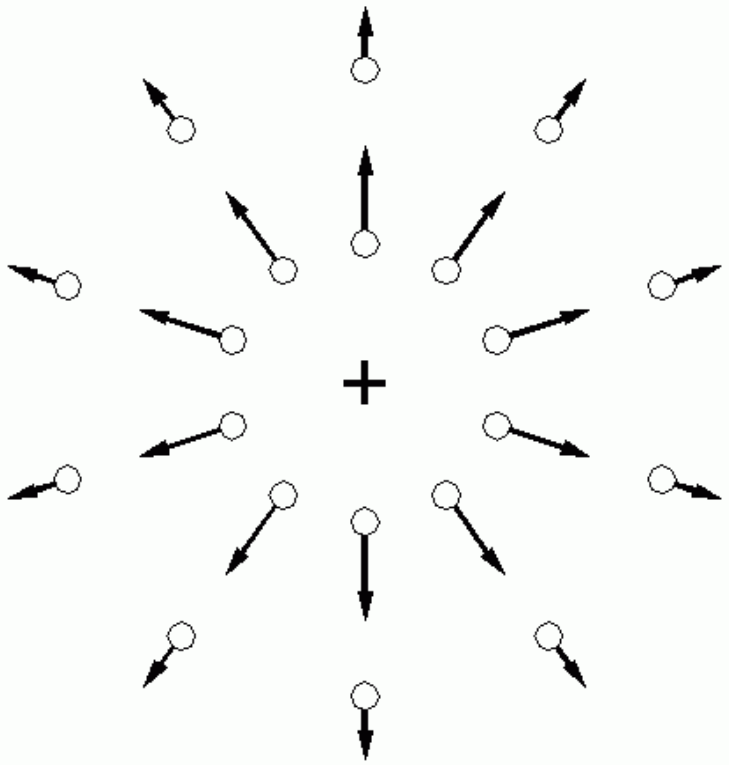

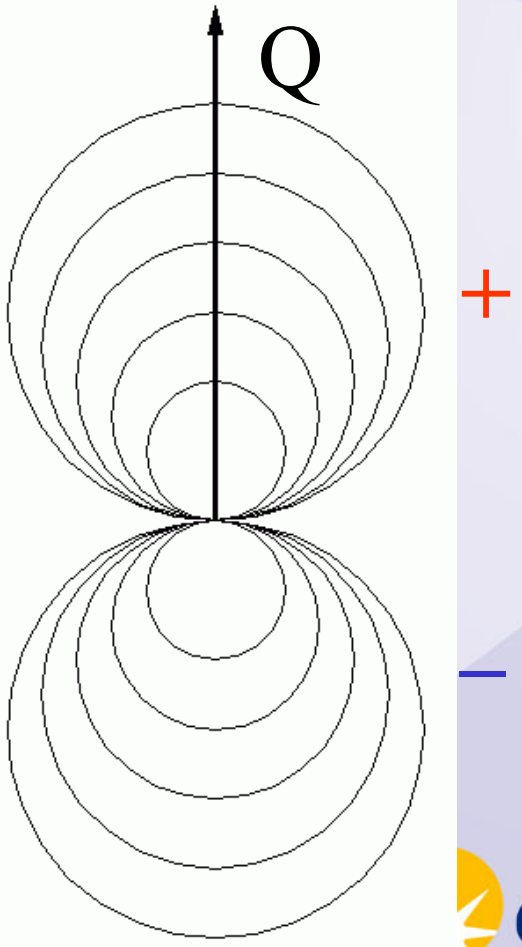

diamond

Good statistics, 3D diffraction data

Mark Pfeifer, Garth Williams, Ivan Vartaniants

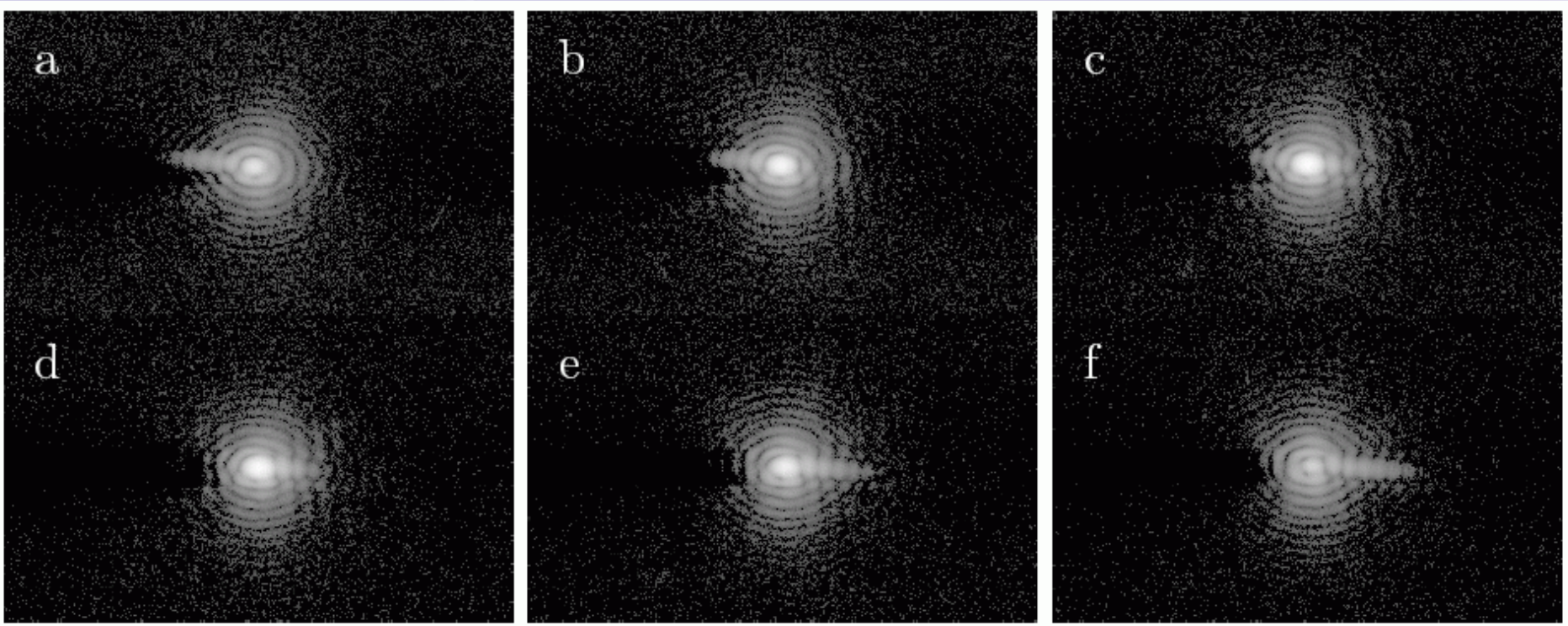

Figure 4.12: Center slices from 3D CXD pattern from Pb sample, on a log scale. Data file 296 from 10/03.

diamond

Facets of Equilibrium Crystal Shape

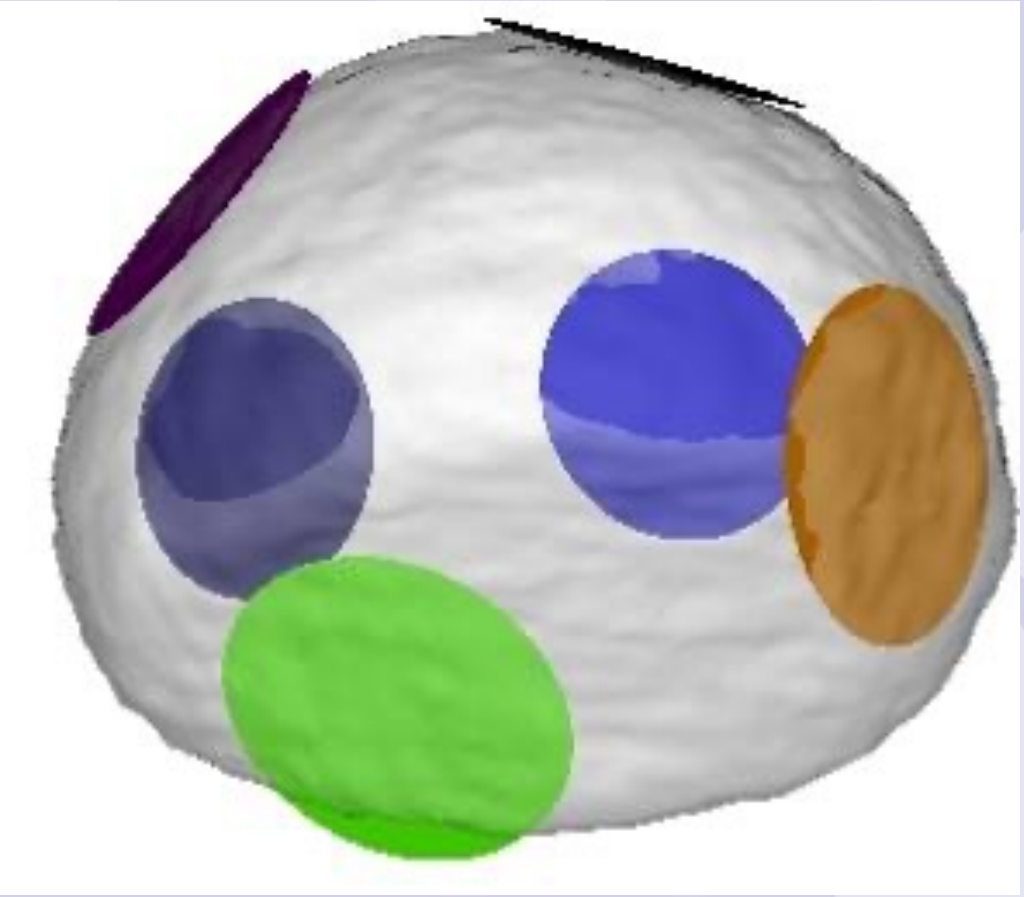

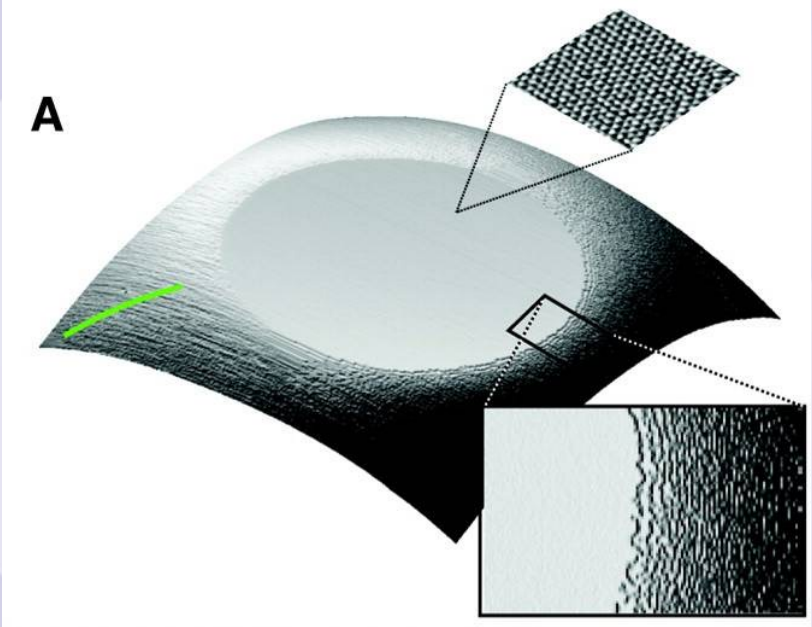

Thurmer K, Williams E, Reutt-Robey J
Science **297** 2033 (2002)

diamond

Modeling of 3D Phase Bump

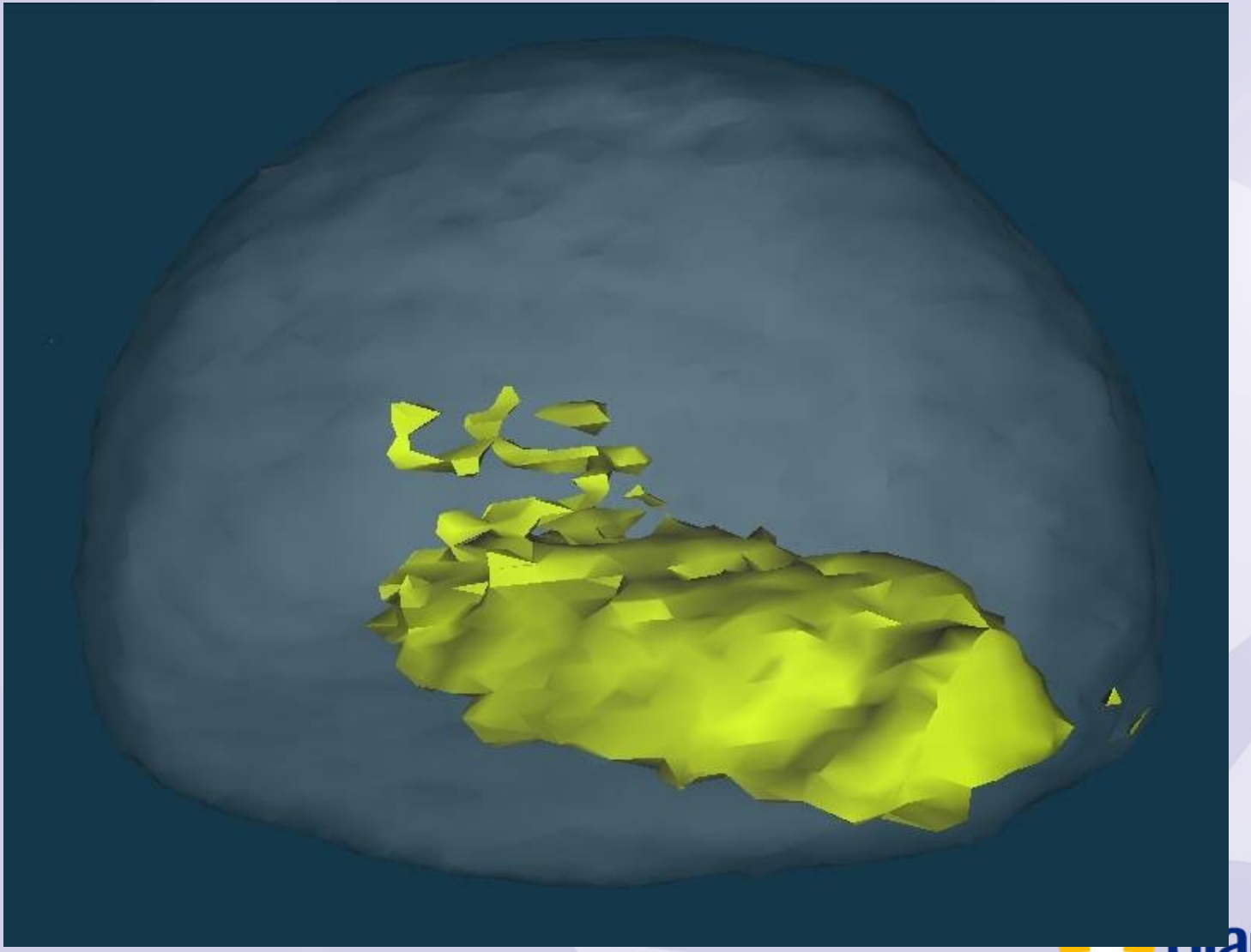

Diamond

3D phase map sections

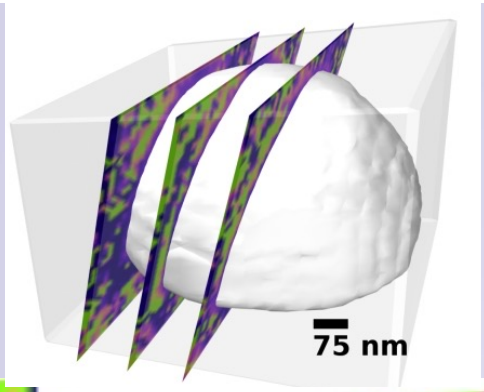

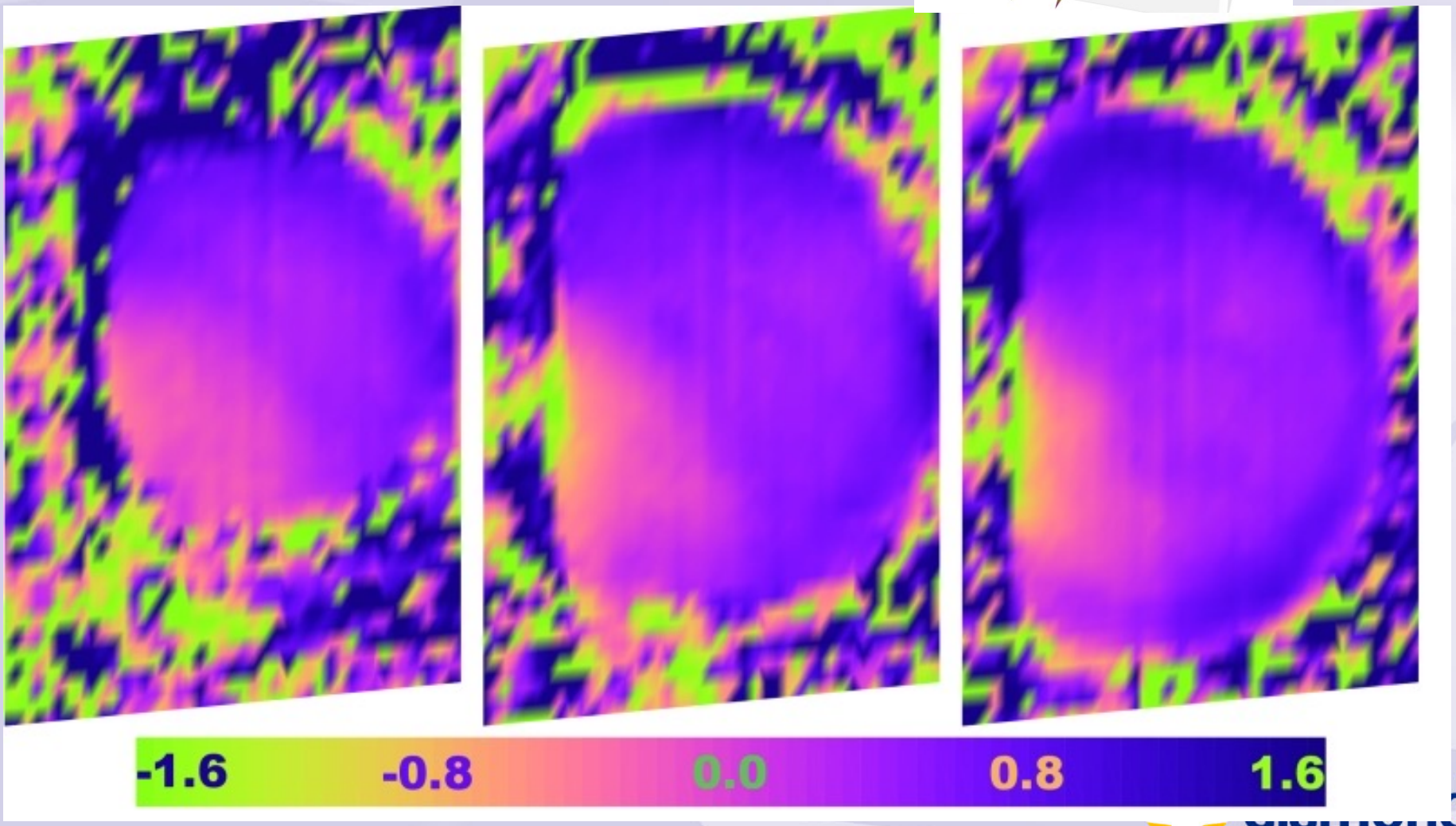

Field lines of Point Charges

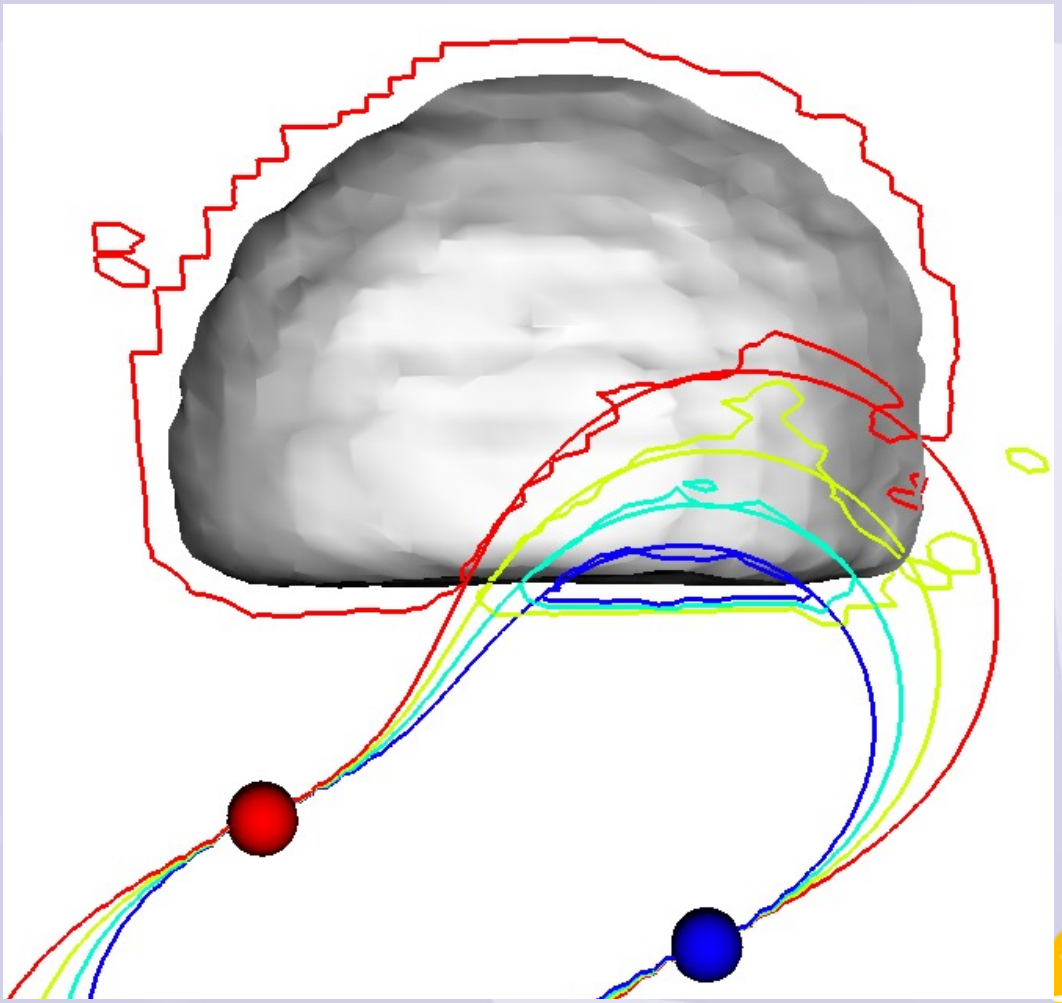

diamond

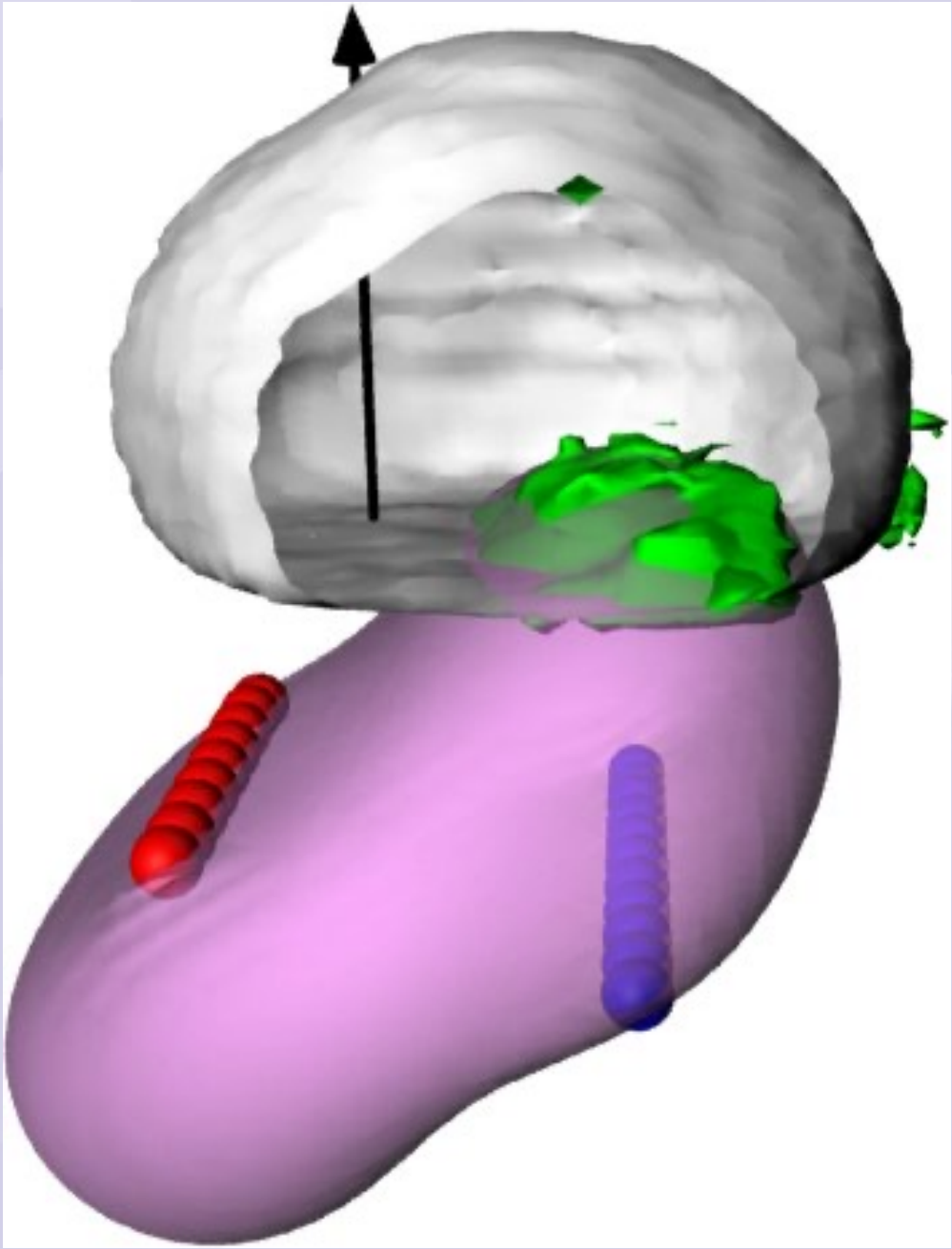

diamond

Contours showing Positive Phase

including correction for refraction by crystal

Ross Harder, PRL (submitted)

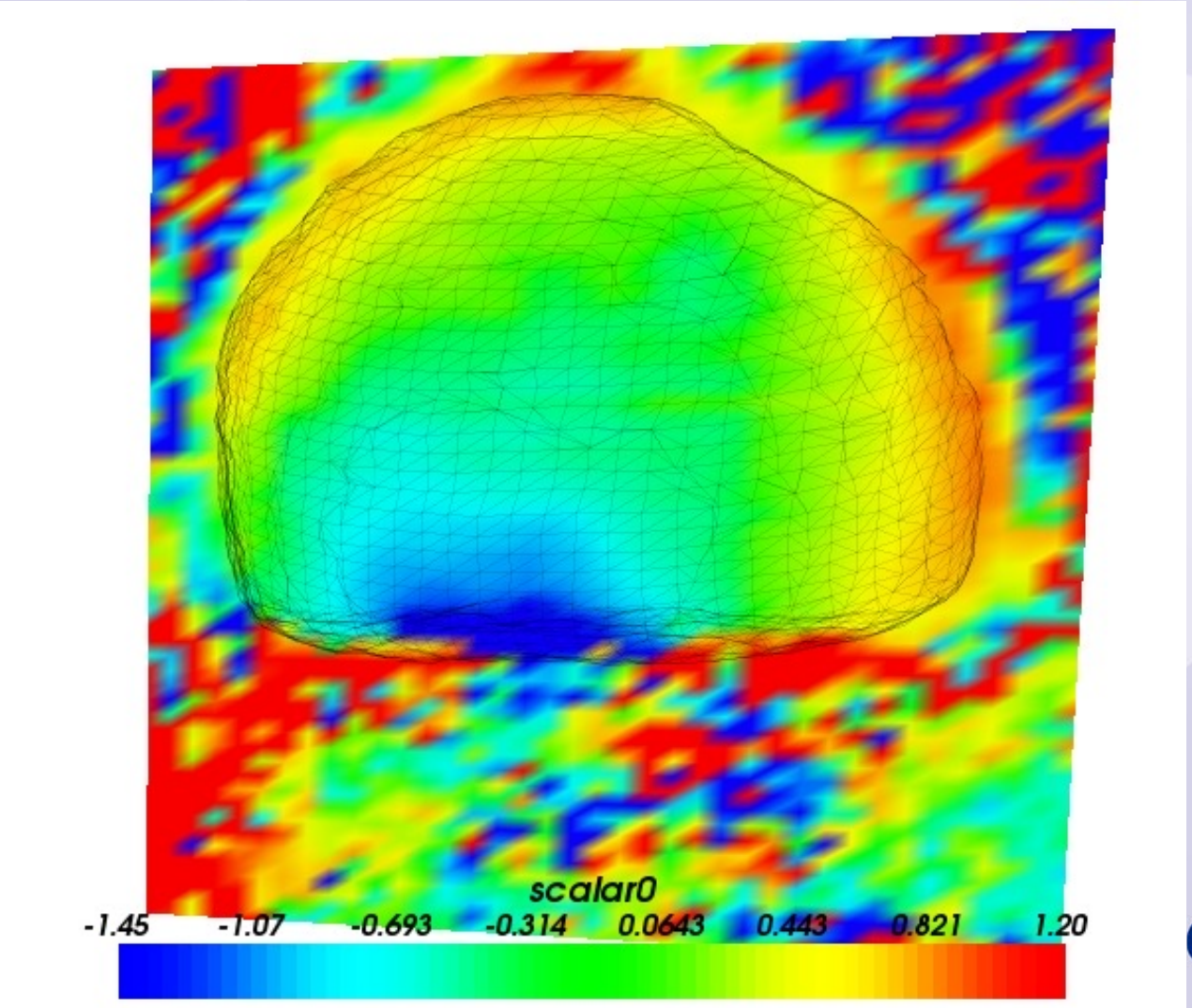

diamond

Depth variation along different azimuths

Exponential depth
90±20nm

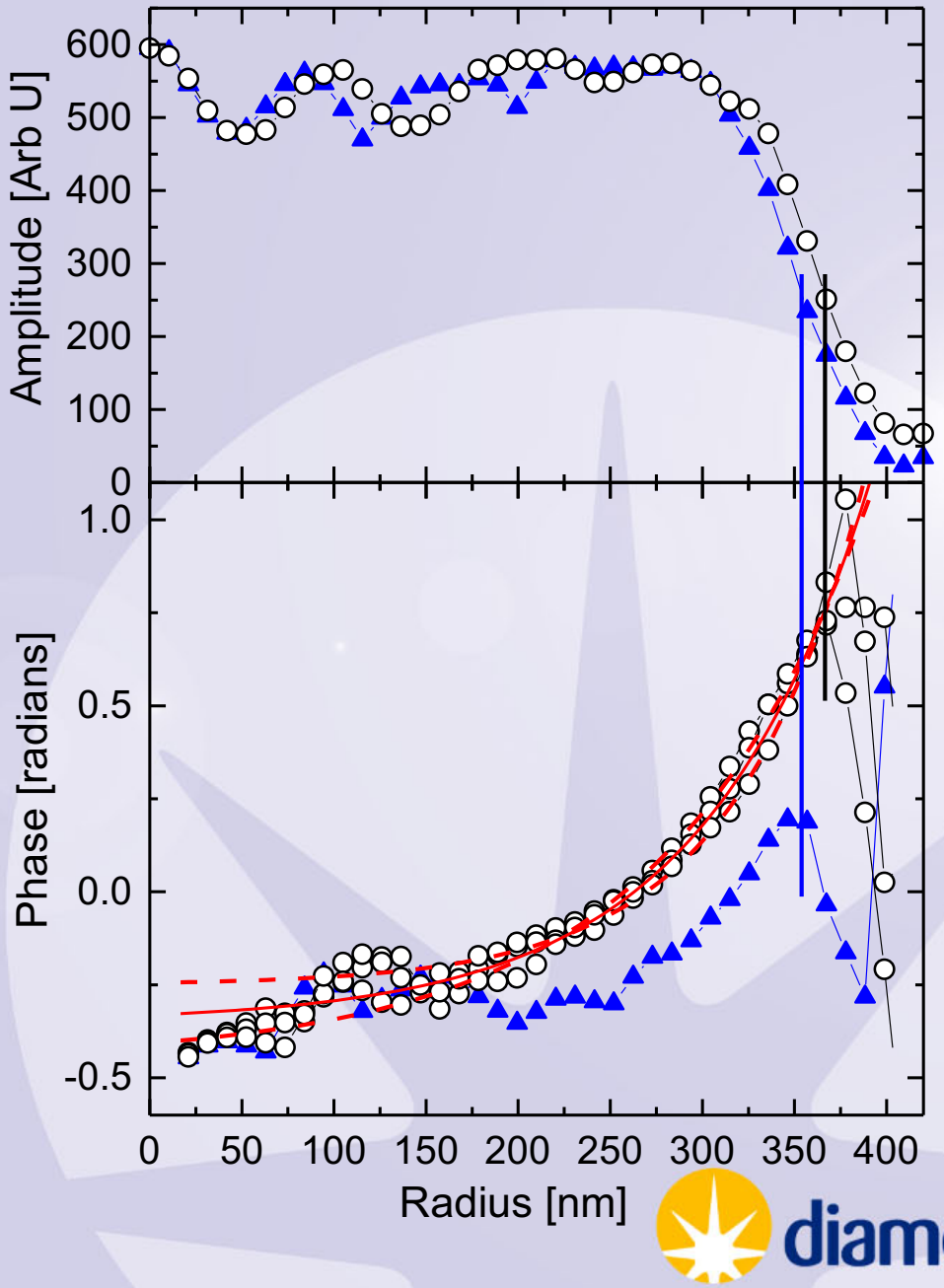

diamond

Conclusions

- Diamond's new capabilities
- Tomography and Phase Contrast
- Typical results
- Angular Rheology of paint
- Inversion of Coherent X-ray Diffraction

diamond